Journal of the American Heart Association

ORIGINAL RESEARCH

Vital Roles of Gremlin-1 in Pulmonary Arterial Hypertension Induced by Systemic-to-Pulmonary Shunts

Liukun Meng, MD; Xiao Teng, MD; Yao Liu, MD; Chao Yang, MD; Shengwei Wang, MD; Wen Yuan, MD; Jian Meng, MD; Hongjie Chi, MD; Lihua Duan, MD; Xiaoyan Liu, PhD

BACKGROUND: Heterozygous mutation in BMP (bone morphogenetic protein) receptor 2 is rare, but BMP cascade suppression is common in congenital heart disease–associated pulmonary arterial hypertension (CHD-PAH); however, the underling mechanism of BMP cascade suppression independent of BMP receptor 2 mutation is unknown.

METHODS AND RESULTS: Pulmonary hypertensive status observed in CHD-PAH was surgically reproduced in rats. Gremlin-1 expression was increased, but BMP cascade was suppressed, in lungs from CHD-PAH patients and shunted rats, whereas shunt correction retarded these trends in rats. Immunostaining demonstrated increased gremlin-1 was mainly in the endothelium and media of remodeled pulmonary arteries. However, mechanical stretch time- and amplitude-dependently stimulated gremlin-1 secretion and suppressed BMP cascade in distal pulmonary arterial smooth muscle cells from healthy rats. Under static condition, gremlin-1 significantly promoted the proliferation and inhibited the apoptosis of distal pulmonary arterial smooth muscle cells from healthy rats via BMP cascade. Furthermore, plasma gremlin-1 closely correlated with hemodynamic parameters in CHD-PAH patients and shunted rats.

CONCLUSIONS: Serving as an endogenous antagonist of BMP cascade, the increase of gremlin-1 in CHD-PAH may present a reasonable mechanism explanation for BMP cascade suppression independent of BMP receptor 2 mutation.

Key Words: BMP cascade ■ congenital heart disease ■ gremlin-1 ■ pulmonary artery hypertension ■ systemic-to-pulmonary shunt

If left untreated, congenital heart diseases associated with systemic-to-pulmonary shunt may expose pulmonary vasculature to persistent flow and pressure overload, subsequently resulting in pulmonary obstructive arteriopathy, increased pulmonary vascular resistance, reversal of systemic-to-pulmonary shunt, and Eisenmenger syndrome.[1] The mechanism of pulmonary obstructive arteriopathy is incompletely elucidated, but studies have confirmed the central roles of excessive proliferation, migration, and apoptosis resistance of pulmonary artery smooth muscle cells (PASMCs) in pulmonary obstructive arteriopathy.[2,3]

Over past decades, the major breakthrough in heritable pulmonary arterial hypertension (PAH) and idiopathic PAH is the identification of BMP (bone morphogenetic protein) signaling reduction caused by the pathogenic mutations of BMP receptor 2 (BMPR2), which subsequently elicits a proproliferative and antiapoptotic status in PASMCs.[4,5] However, as a special form of PAH, congenital heart disease–associated PAH (CHD-PAH) carries the lowest level of BMPR2 mutation but common suppression of BMP cascade in lungs,[6–9] even in rat or piglet lungs exposed to systemic-to-pulmonary shunts,[10–12] thus implicating the more common BMP cascade suppression independent of

Correspondence to: Lihua Duan, MD, Department of Rheumatology and Immunology, Jiangxi Provincial People's Hospital, Nanchang, Jiangxi 330006, China. E-mail: lh-duan@163.com and Xiaoyan Liu, PhD, Medical Research Center, Beijing Chao-Yang Hospital, 8 Gongren Tiyuchang Nanlu, Chaoyang District, Beijing 100020, China. E-mail: lxy-213@163.com

Supplementary materials for this article are available at https://www.ahajournals.org/doi/suppl/10.1161/JAHA.120.016586

For Sources of Funding and Disclosures, see page 16.

JAHA is available at: www.ahajournals.org/journal/jaha

CLINICAL PERSPECTIVE

What Is New?

- Systemic-to-pulmonary shunt time dependently upregulated gremlin-1 level in lungs.
- Mechanical stretch promoted gremlin-1 expression in distal pulmonary arterial smooth muscle cells, which exerts promoting roles in distal pulmonary arterial smooth muscle cell phenotype change, partially mediated by BMP (bone morphogenetic protein) cascades.
- Serum gremlin-1 levels correlated with the severity of systemic-to-pulmonary shunt–associated pulmonary arterial hypertension.

What Are the Clinical Implications?

- Gremlin-1 may be a potential biomarker and therapeutic target for patients with congenital heart disease–associated pulmonary arterial hypertension.

Nonstandard Abbreviations and Acronyms

Bcl-2	B-cell lymphoma-2
BMP-2	bone morphogenetic protein-2
BMPR2	bone morphogenetic protein receptor 2
CHD-PAH	congenital heart disease–associated pulmonary arterial hypertension
CSG-12W	combined surgery group reserving for 12 weeks
CSG-8W	combined surgery group reserving for 8 weeks
CSG-CSL	combined surgery group receiving cervical shunt ligation at the postoperative eighth week and continuously kept for the subsequent 4 weeks
dPASMC	distal pulmonary arterial smooth muscle cell
Id1	inhibitor of DNA-binding 1
IED	in external diameter
mPAP	mean pulmonary arterial pressure
PAEC	pulmonary arterial endothelial cell
SOG	sham operation group
VSMC	vascular smooth muscle cell

BMPR2 mutation in CHD-PAH. Nonetheless, the potential mechanism remains elusive.

Recent studies have found that BMP antagonist, gremlin-1, is significantly increased in hypoxia PAH, whereas knockout or blockage of gremlin-1 attenuates hypoxia or hypoxia/SU5416-induced PAH.[13,14] Parallel data have also revealed that mechanical injury incurred gremlin-1 promotes systemic artery remodeling[15]; thus, we hypothesized that systemic-to-pulmonary shunt increases gremlin-1 expression in lungs participating in pulmonary obstructive arteriopathy, thus presenting a mechanistic explanation for BMP cascade reduction in CHD-PAH independent of BMPR2 mutations. Therefore, the aim of this study was to investigate the role of gremlin-1 in CHD-PAH using our previously published rat PAH model.

METHODS

The data that support the findings of this study are available from the corresponding author on reasonable request.

Study Design of Gremlin-1 in Human Samples

Clinical characteristics and grouping of subjects included in this protocol have been presented in detail in our previous report.[10] This part of the study complied with the principles summarized in the Declaration of Helsinki and authorized by the "Research Ethics Committee of Fuwai Hospital, Chinese Academy of Medical Sciences and Peking Union Medical College" (No. 2009-229). All participants provided informed written consent.

Briefly, patients with CHD were divided into 3 groups: no PAH group (CHD–non-PAH, n=18, pulmonary vascular resistance ≤3 Wood), severe PAH group (n=20, 3 Wood<pulmonary vascular resistance<10 Wood), and Eisenmenger syndrome group (n=27, pulmonary vascular resistance ≥10 Wood). Patients with CHD–non-PAH or CHD–severe PAH all presented persistent systemic-to-pulmonary shunt, whereas patients with CHD– Eisenmenger syndrome demonstrated reversed pulmonary-to-systemic shunt or bidirectional shunt. Hemodynamic parameters derived from routine right heart catheterization procedures were collected. Blood specimens were taken from patients with CHD and age- and sex-matched control subjects (n=21, Table 1). Otherwise, control lung explants (n=5) were dissected from normal regions at least 5 cm away from neoplasm margins during lung cancer surgery. Hypertensive lung tissues in the peripheral region were harvested during heart-lung transplantation for Eisenmenger syndrome (n=5).

Flow and Pressure Overload in Pulmonary Circulation Surgically Induced by Systemic-to-Pulmonary Shunts in Rats

The experimental protocols were authorized by the Ethics Committee on Animal Study of Fuwai Hospital

Table 1. Demographics of Patients Involved in This Study

Parameter	Control	CHD–non-PAH	CHD-sePAH	CHD-ES
No. of patients	21	18	20	27
Age, y	27 (22–44)	34.5 (26–49)	32 (23.5–38)	27 (20–36)
Sex (men/women), %	52.38/47.62	50/50	35/65	18.52/81.48
Diagnosis				
ASD/VSD/PDA, %	0/0/0	27.78/38.89/33.33	25/35/40	33.33/40.74/25.93
Hemodynamic indexes				
PASP, mm Hg		38.56±9.00	80.70±21.82	114.22±15.05
mPAP, mm Hg		23.17±7.29	53.05±15.16	82.26±12.88
CO, L/min		8.08±2.18	6.67±2.00	4.07±1.70
CI, L/min per m^2		5.00±1.56	4.25±1.40	2.70±1.17
PVR, Wood		1.99±0.88	6.63±1.98	20.37±7.52
TPVR, Wood		3.17±0.70	8.27±2.13	23.32±7.85
Gremlin-1, ng/mL	82.02±20.65	140.99±30.61	253.12±47.82	313.52±62.15

Age data are presented as median (interquartile range), and hemodynamic data are presented as mean±SD. ASD indicates atrial septal defect; CHD, congenital heart disease; CHD-ES, CHD patients with Eisenmenger syndrome; CHD–non-PAH, CHD patients with no PAH; CHD-sePAH, CHD patients with severe PAH; CI, cardiac index; CO, cardiac output; mPAP, mean pulmonary arterial pressure; PAH, pulmonary arterial hypertension; PASP, pulmonary arterial systolic pressure; PDA, patent ductus arteriosus; PVR, pulmonary vascular resistance; TPVR, total pulmonary vascular resistance; and VSD, ventricular septal defect.

(approval No. 0000502) and implemented according to the *Guide for the Care and Use of Laboratory Animals* (NIH publication No. 85-23; National Academy Press, Washington, DC; revised 2011).

Forty Sprague-Dawley rats (male, 6 weeks old, 200±10 g) were purchased from Vital River Laboratory Animal, Inc (Beijing, China), and randomly assigned to the sham operation group (SOG; n=10) and combined surgery group (CSG; n=30). Female rats were not used to eliminate the possible effect of estrogen on PAH.[1] As demonstrated in the grouping flow chart (Figure S1), 10 rats from CSG were kept for 8 weeks (CSG-8W; n=10), 10 rats from CSG were kept for 12 weeks (CSG-12W; n=10), and 10 received surgically cervical shunt ligation at the eighth week and were continuously kept for the subsequent 4 weeks (CSG-CSL; n=10). Surgeries were performed under the combined anesthesia by isoflurane anesthesia (1.5% vol/vol) and buprenorphine hydrochloride (0.03 mg/kg), as described in our previous research.[16] In brief, combined surgeries were composed of 2 sequentially surgical procedures with 1-week interval (ie, right pulmonary artery ligation [right posterolateral thoracotomy through the third intercostal space] and a cervical systemic-to-pulmonary shunt [left common carotid artery to external jugular vein]). At the same time, the sham operation was also performed in a 2-stage surgical procedure without ligation of right pulmonary arteries and the construction of left cervical shunts.

Postoperatively, all rats were kept under a normal light cycle with constant temperature (21°C) and relative humidity (50%–70%), and were routinely provided with standard laboratory chow, water, and prophylactic medicines (aspirin and hydrochlorothiazide), as we previously reported.[10,16]

Right Heart Catheterization in Rats

At the harvesting time points, the right heart catheterization procedure was performed by an investigator blinded to the animal grouping and experimental protocol in a closed-chest manner, as previously reported.[10,16] Briefly, after right heart catheter was localized in the right ventricle, and main pulmonary artery trunk, and after 5 minutes stabilization, mean values were recorded and analyzed for right ventricular systolic pressure, right ventricular developed pressure, pulmonary arterial systolic pressure, pulmonary artery diastolic pressure, mean pulmonary arterial pressure (mPAP), and the positive and negative maximum of right ventricular pressure. Meanwhile, systolic blood pressure of the systemic circulation and mean systemic blood pressure were also measured via the left femoral artery, and ratios of pulmonary arterial systolic pressure/systolic blood pressure and mPAP/mean systemic blood pressure were calculated. Data obtained in all rats survived until the right heart catheterization was included in the final statistical calculation. One rat in CSG-8W that died because of unknown reasons was excluded.

Rat Sample Harvesting

As previously reported,[10] vein blood samples (0.5 mL) were acquired via inferior vena cava after right heart catheterization. Plasma was immediately centrifuged for 15 minutes at 1710*g* and 4°C, and then aliquoted

and frozen at –80°C for further gremlin-1 detection using ELISA.

After right heart catheterization, the left lung and heart were perfused to pink white with 4°C physiological saline via inferior cava vena with abdominal aorta being cut off, after which the left lung was extirpated, placed on ice, and further dissected into 2 parts. The superior part was snap frozen in liquid nitrogen for real-time polymerase chain reaction and Western blotting analysis, and the inferior part was routinely immersed into 10% neutral-buffered formalin, trimmed into tissue block, and processed for paraffin embedding. Otherwise, right ventricular hypertrophy was analyzed by the ratio of the wet weight of right ventricle/that of the left ventricle plus septum.[16]

Histological Analysis

Our previous studies confirmed that pulmonary vasculopathy in PAH induced by combined surgery is mainly localized in distal pulmonary arteries <75 μm in external diameter (IED).[10,16] To clearly define the grade of pulmonary vasculopathy (muscularization, medial hypertrophy, and luminal occlusion) in distal pulmonary arteries <75 μm IED, two 5-μm lung sections from each rat were stained: one was stained with hematoxylin-eosin staining to manifest cells, whereas the other was initially stained with the Weigert method and then with the Van Gieson solution to differentiate the 3 layers with different colors. Evaluation of pulmonary vasculopathy in distal pulmonary arteries <75 μm IED in each slide was performed by one investigator blinded to animal grouping and experimental protocol.

Pulmonary vasculopathy in distal pulmonary arteries <75 μm IED was carefully graded, referencing the classification proposed by Heath-Edwards and Wagenvoort[17,18] (ie, media muscularization without intimal cellular proliferation or intimal fibrosis [grade I], medial hypertrophy with cellular intimal proliferation [grade II], or cellular or fibrous vascular occlusion [grade III]). Quantitative analysis of muscularization, medial hypertrophy, and luminal occlusion in distal pulmonary arteries <75 μm IED are described in detail in our previous reports.[10,16]

RNA Isolation and Real-Time Polymerase Chain Reaction Analysis

Frozen lung tissue and rat distal PASMCs (dPASMCs) were homogenized and total RNA was isolated with TRIzol reagent (Invitrogen, Carlsbad, CA) and reverse transcribed to cDNA using an AMV Reverse Transcriptase Kit (Promega, Madison, WI). Transcription levels of gremlin-1, BMPR2, inhibitor of DNA-binding 1 (Id1), Bax, B-cell lymphoma-2 (Bcl-2), and GAPDH were detected with SYBR Green PCR MasterMix in a 7300 Fast Real-Time PCR System (Applied Biosystems, Foster City, CA) with duplicate experimental samples for each sample, and normalized by GAPDH amplified from the same samples and served as the internal control. The sequences of primers for gremlin-1, BMPR2, Id1, Bax, Bcl-2, and GAPDH are presented in Table 2.

Western Immunoblotting Analysis

The Western blotting analysis was performed on lung tissues and whole protein lysates of dPASMCs, as described in our previous report.[10] In brief, after extraction with lysis buffer and quantification with a BCA protein assay kit (Pierce, Rockford, IL), protein extracts (40 μg per sample) were separated with 4% to 12% (vol/vol) gradient SDS-PAGE, blocked for 2 hours in tris-buffered saline containing 0.1% (vol/vol) Tween-20 and 10% (wt/vol) nonfat dry milk powder. After incubation with primary antibodies (overnight at 4°C) and secondary antibodies (1 hour at room temperature), signal densitometry of target protein band was detected with an ECL chemiluminescence detection kit (PK-MB902-500-500; PromoCell, Germany) and quantified using ImageJ software. The value was normalized to GAPDH of each loading control. Primary antibodies used in this study are listed in Table 3.

Immunohistochemistry and Immunofluorescence Staining for Gremlin-1 in Lungs

Immunohistochemistry Staining for Gremlin-1 in Human Lungs

As we previously reported,[10] after serial pretreatment of deparaffinization, rehydration, antigen retrieval (100℃ citrate buffer, pH 6.0, 20 minutes), permeabilization (0.3% Triton X-100 in PBS), and nonspecific binding blocking (5% normal goat serum), human lung sections were immunostained with gremlin-1 primary antibody (Table 3) overnight at 4°C, then sequentially hybridized with biotinylated secondary antibody, horseradish peroxidase–conjugated streptavidin, and final 3, 3'-diaminobenzidine. Gremlin-1 immunoreactivity was routinely analyzed by the Olympus imaging analyzer system (BX61; Tokyo, Japan).

Immunofluorescence Staining for Gremlin-1 in Rat Lungs

After the routine serial pretreatment that was performed as aforementioned, rat lung sections (5 μm) were incubated with primary antibodies to gremlin-1 in the presence of endothelial marker von Willebrand factor or smooth muscle cell marker smooth muscle α-actin at 4°C overnight, then were hybridized with secondary antibodies at room temperature for 1 hour, further counterstained with 4′6-diamidino-2-phenylindole (1:1000;

Table 2. Primer Sequences for Real-Time PCR

Gene	Forward 5′-3′	Reverse 5′-3′
Gremlin-1 (r)	CCTTTCTTTGCTCTCCCTGA	TTGTCTCCCCACACTCTGAA
BMPR2 (r)	CCGGGCAGGATAAATCAGGA	ATTCTGGGAAGCAGCCGTAG
Id1 (r)	GAACCGCAAAGTGAGCAAGG	GAACCGCAAAGTGAGCAAGG
GAPDH (r)	GGCACAGTCAAGGCTGAGAATG	ATGGTGGTGAAGACGCCAGTA
Bax (r)	CGTGGTTGCCCTCTTCTACT	TCACGGAGGAAGTCCAGTGT
Bcl-2 (r)	GTGGACAACATCGCTCTGTG	CATGCTGGGGCCATATAGTT
Gremlin-1 (h)	GCAAATACCTGAAGCGAGAC	CGATGGATATGCAACGACAC
GAPDH (h)	ACCACAGTCCATGCCATCAC	TCCACCACCCTGTTGCTGTA

Bcl-2 indicates B-cell lymphoma-2; BMPR2, BMP (bone morphogenetic protein) receptor 2; h, Homo sapiens; Id1, inhibitor of DNA-binding 1; PCR, polymerase chain reaction; and r, Rattus norvegicus.

Sigma-Aldrich, St. Louis, MO), and finally mounted with fluorescence antifading solution (Vectashield; Vector Labs, CA). Fluorescence images were analyzed with a Leica SP8 confocal laser scanning microscope.

Cell Culture

Rat dPASMCs from peripheral pulmonary tissue explants of healthy rats were harvested and cultured, as previously reported.[11] All dPASMCs used for in vitro functional studies were passages between 4 and 6.

Detection of Cell Cycle Distribution by Flow Cytometry

The cell cycle phase distribution of dPASMCs was determined by flow cytometry. First, dPASMCs were synchronically starved in serum-reduced media (0.4% fetal bovine serum) for 48 hours, then culture media were replaced with complete smooth muscle cell medium for the indicated time (0, 12, or 24 hours). After trypsinization, harvested dPASMCs were centrifuged at 800*g* for 5 minutes at 4℃, resuspended in fluorescence-activated cell sorting buffer (100 mmol/L sodium acetate and 5.4 mmol/L EDTA, pH 5.2), fixed in 70% ethanol overnight at 4°C, and finally permeabilized with 0.2% Triton X-100 for 30 minutes. For DNA staining, dPASMCs were then incubated with Rnase A (50 μg/mL) and propidium iodide (100 μg/mL; Sigma-Aldrich) at room temperature for 30 minutes in the dark. After these sequential pretreatments, the DNA content of dPASMCs was assessed by flow cytometry (FACSAria; Becton Dickinson, San Jose, CA). Results were expressed as percentage of cells in each cell cycle phase. The experiments were performed in triplicate.

dPASMC Mechanical Stretch

For stretch experiments, dPASMCs were transferred to the Bioflex plates (BioFlex Flexcell International

Table 3. List of Primary Antibodies Used in This Study

Catalog No.	Clonality	Manufacturer	Antibody (SR)	Dilution
sc-515877	Mouse-monoclonal	Santa Cruz Biotechnology (CA, USA)	Gremlin-1 (rat)	1:200 (Immunofluorescence)
Ab157576	Rabbit-polyclonal	Abcam (Cambridge, UK)	Gremlin-1 (rat)	1:400 (WB)
AF956	Goat-polyclonal	R&D Systems (Minneapolis, MN)	Gremlin-1 (human)	1:200 (Immunohistochemistry)
sc-515877	Mouse-monoclonal	Santa Cruz Biotechnology (CA, USA)	Gremlin-1 (human)	1:1000 (WB)
sc-32233	Mouse-monoclonal	Santa Cruz Biotechnology (CA, USA)	GAPDH (rat, human)	1:1000 (WB)
G9545	Rabbit-polyclonal	Sigma-Aldrich (St. Louis, MO)	GAPDH (rat, human)	1:2000 (WB)
ab7817	Mouse-monoclonal	Abcam (Cambridge, UK)	α-SMA (rat)	1:100 (Immunofluorescence)
ab6994	Rabbit-polyclonal	Abcam (Cambridge, UK)	vWF (rat)	1:100 (Immunofluorescence)
ab130206	Mouse-monoclonal	Abcam (Cambridge, UK)	BMPR2 (rat)	1:1000 (WB)
ab230679	Rabbit-polyclonal	Abcam (Cambridge, UK)	Id1 (rat)	1:1000 (WB)
13820	Rabbit-monoclonal	Cell Signaling Technology (Danvers, MA)	P-Smad1/5/8 (rat)	1:1000 (WB)
21684	Rabbit-polyclonal	Signalway Antibody (MD, USA)	Smad1/5/8 (rat)	1:1000 (WB)
ab32503	Rabbit-monoclonal	Abcam (Cambridge, UK)	Bax (rat)	1:2000 (WB)
ab196495	Rabbit-polyclonal	Abcam (Cambridge, UK)	Bcl-2 (rat)	1:2000 (WB)

Bcl-2 indicates B-cell lymphoma-2; BMPR2, BMP (bone morphogenetic protein) receptor 2; Id1, inhibitor of DNA-binding 1; P-Smad1/5/8, phosphorylated Smad1/5/8; α-SMA, smooth muscle α-actin; Smad1/5/8, drosophila mothers against decapentaplegic protein 1/5/8; SR, species reactivity; vWf, von Willebrand factor; and WB, Western blotting.

Corporation, Hillsborough, NC) at a density of 1×10^5 cells/well with 2 mL complete smooth muscle cell medium per well and allowed to adhere for 48 hours. Subsequently, complete smooth muscle cell medium was replenished with basic smooth muscle cell medium (0.4% fetal bovine serum) and dPASMCs were starved for 48 hours to induce quiescence. Thereafter, arresting dPASMCs were cultured in fresh complete smooth muscle cell medium and subjected to mechanical stretch by using the Flexcell FX-5000 tension system (Flexcell International Corp). To determine the duration of applied stretch necessary to produce changes in the expression of gremlin-1, BMPR2, and Id1, dPASMCs were subjected to stretch at 1 Hz at the amplitude of 15% for 6, 12, 24, and 48 hours. To determine the appropriate stretch amplitude necessary to incur changes in the expression of gremlin-1, BMPR2, and Id1, dPASMCs were stretched at a frequency of 1 Hz for 24 hours at amplitudes of 5%, 10%, 15%, and 20%. After this, the suitable duration and amplitude of optimal stretch with the maximum effect were chosen. Thereafter, the optimal effect of mechanical stretch on the protein level of gremlin-1 and BMP cascade were further analyzed. Control dPASMCs from the same batch as stretch group were statically cultured in BioFlex plates and were subjected to the sequential culture procedure but were not exposed to mechanical stretch.

dPASMC Proliferation Assay

The proliferation of dPASMCs from healthy rats was determined using 5-bromo-2-deoxy-uridine incorporation assay (Calbiochem, Gibbstown, NJ) following the provided protocol.

First, a total of 1×10^4 dPASMCs were seeded into each well of a 96-well plate in 100 mL complete smooth muscle cell medium. After overnight attachment and subsequent arresting with low serum starvation (0.4% fetal bovine serum) for 48 hours, synchronized dPASMCs were treated with complete smooth muscle cell medium containing recombinant BMP2/4 (355-BM, 5020-BP; R&D Systems, Minneapolis, MN), BMP2/4+gremlin-1 (956-GR; R&D Systems), and BMP2/4+gremlin-1+anti–gremlin-1 (AF956; R&D Systems) at indicated concentrations and were incubated for different time intervals. Six hours before incubation termination, 5-bromo-2-deoxy-uridine (10 mL) was added into each well. Subsequently, dPASMCs were fixed, incubated with anti–5-bromo-2-deoxy-uridine antibody, and finally quantified by measuring the absorbance at 450 nm with a microplate reader (Mode 680; Bio-Rad, Tokyo, Japan), as we previously reported.[10] Proliferation rates of dPASMCs were presented as relative folds to the mean value of the control dPASMCs. Experiments were all performed in triplicate.

dPASMC Apoptosis Detection

Apoptosis rates of dPASMCs were detected by Annexin V/PI staining assay kit, according to the manufacturer's protocol (BD Biosciences, Oxnard, CA). Briefly, after pretreatment with BMP2/4, BMP2/4+gremlin-1, BMP2/4+gremlin-1+anti–gremlin-1 at indicated concentrations, dPASMCs were trypsinized, washed in ice-cold PBS, and labeled with annexin V–fluorescein isothiocyanate in the dark. Then, the nuclei were stained with 10 mg/mL 4′, 6′-diamidino-2-phenylindole dihydrochloride for 10 minutes at 20°C. Finally, samples were detected using the FACSCanto II flow cytometer (BD Biosciences) within 1 hour and analyzed by Flowjo software.

Detection of Plasma Gremlin-1 Concentration

Human and rat plasma concentrations of gremlin-1 were detected by commercially available ELISA kits (NBP2-75362, NBP2-75364; Novus Biologicals, LLC), according to the manufacturer provided protocols. The duplicate assay was performed in all the standards and samples, and the mean values were analyzed. A microplate reader (Mode 680; Bio Rad, Tokyo, Japan) was used to measure the absorbance at 450 nm. Plasma concentrations of gremlin-1 were calculated using a standard curve constructed by titrating standards.

Statistical Analysis

Data are all expressed as mean±SD of at least 4 independent experiments. Statistical analysis was performed using SPSS 13.0 statistics software. Comparisons between 2 groups were evaluated using Student *t* test. Differences among groups were tested by 1-way ANOVA. Nonparametric tests were used for nonnormally distributed values. The correlation between plasma gremlin-1 concentration and hemodynamic values in rats was analyzed by linear regression analysis. $P<0.05$ was considered to be statistically significant.

RESULTS

Systemic-to-Pulmonary Shunt Time-Dependently Incurred Apparent Pulmonary Hypertensive Status in Rats

As demonstrated in Figure 1A through 1J, after exposure to systemic-to-pulmonary shunt for 8 or 12 weeks, baseline level of right ventricular systolic pressure, right ventricular developed pressure, the positive and negative maximum of right ventricular pressure, ratio of the wet weight of right ventricle/that of the left ventricle plus septum, pulmonary arterial systolic pressure,

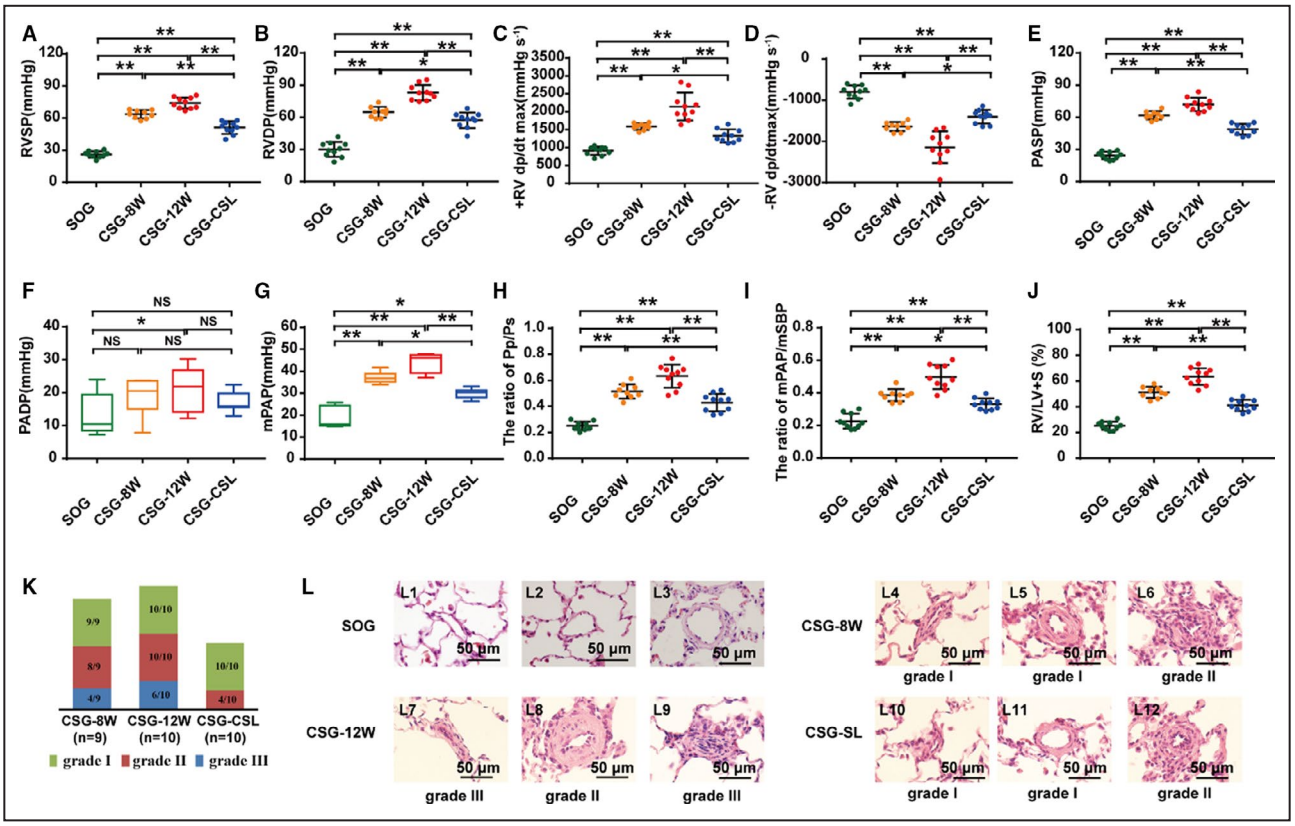

Figure 1. Pulmonary hypertensive status in rats with persistent systemic-to-pulmonary shunt or cervical shunt ligation. **A** through **J**, Hemodynamic indexes derived from right heart catheterization procedure and ratio of the weight of right ventricle/that of left ventricle plus septum (RV/LV+S). **A**, Right ventricular systolic pressure (RVSP). **B**, Right ventricular developed pressure (RVDP). **C**, Positive maximum RV dP/dt (+RV dp/dtmax). **D**, Negative maximum RV dP/dt (–RV dp/dtmax). **E**, Pulmonary arterial systolic pressure (PASP). **F**, Pulmonary artery diastolic pressure (PADP). **G**, Mean pulmonary arterial pressure (mPAP). **H**, Ratio of pulmonary arterial systolic pressure/systemic arterial systolic pressure (Pp/Ps). **I**, mPAP/mean systemic blood pressure (mSBP). **J**, RV/LV+S. **K**, Proportion of pulmonary vasculopathies of different grades presented in intra-acinar pulmonary arteries <50 μm in external diameter. **L**, Representative morphological imagines of pulmonary arterioles (hematoxylin-eosin stain, ×1000). L1 to L3, Intra-acinar pulmonary arteries from sham operation group (SOG) with normal morphological features; L4 to L6, intra-acinar pulmonary arteries from combined surgery group reserving for 8 weeks (CSG-8W) with severe muscularization (L4-L5) and cellular intimal proliferation (L6); L7 to L9, intra-acinar pulmonary arteries from combined surgery group reserving for 12 weeks (CSG-12W) with muscularization (L7-L8) and neointima formation and cellular luminal occlusion (L7 and L9); and L10 to L12, intra-acinar pulmonary arteries from combined surgery group receiving cervical shunt ligation at the postoperative eighth week and continuously kept for the subsequent 4 weeks (CSG-CSL) with slight muscularization (L10-L12) and intimal proliferation with patent lumen (L12). Data are mean±SD. n=9 to 10 rats per group. NS indicates not significant. **P*<0.05, ***P*<0.01, and NS *P*>0.05.

mPAP, pulmonary arterial systolic pressure/systolic blood pressure, and mPAP/mean systemic blood pressure, observed in SOG, increased over time to a much higher level, as shown in CSG-8W and CSG-12W. After cervical shunt ligation, these parameters decreased to a much lower level, as detected in CSG-CSL (all *P*<0.01), which indicated that systemic-to-pulmonary shunt time-dependently deteriorated pulmonary hypertensive status, whereas the correction of cervical shunt facilitated the regression of PAH.

Furthermore, as presented in Figure 1K and 1L, 8 weeks' exposure to systemic-to-pulmonary shunt induced pulmonary vasculopathy of grade I (muscularization, 9/9), grade II (cellular intimal proliferation, 5/9), and grade III (intimal fibrosis and entirely luminal occlusion, 3/9) in CSG-8W, whereas 12 weeks' exposure induced pulmonary vasculopathy of grade I (10/10), grade II (10/10), and grade III (6/10) in CSG-12W, but pulmonary vasculopathies observed in CSG-8W regressed to a much remissive status (ie, grade I [10/10], grade II [4/10], and grade III [0/10]) after cervical shunt ligation in rats of CSG-CSL. Distribution diversity in the extent of pulmonary vasculopathy among the above groups suggested that systemic-to-pulmonary shunt incurred pulmonary vasculopathy of grade I to III over time, which could be partially reversed after surgical ligation of the cervical shunt.

Systemic-to-Pulmonary Shunt Time-Dependently Inhibited BMP Cascade But Increased Gremlin-1 Level in Rat Lungs

Compared with those of SOG, protein levels of BMPR2, P-Smad1/5/8 (phosphorylated drosophila mothers against decapentaplegic protein 1/5/8), and BMP-targeted intranuclear gene transcription of Id1 decreased time-dependently in rat lungs (Figure 2A through 2D). However, corresponding to the interval through which rat lungs experienced systemic-to-pulmonary shunts, mRNA level of gremlin 1 in rat lungs from CSG-8W and CSG-12W gradually increased, which indicated that increased gremlin-1 level was a persistent response to pressure and flow overload in the pulmonary circulation (Figure S2, Figure 2A and 2E).

Gremlin-1 Increase and BMP Cascade Suppression Partially Recovered After Cervical Shunt Ligation

As expected, the expression levels of BMP cascade (BMPR2, P-Smad1/5/8, and Id1) were also downregulated in the lungs of CSG-CSL compared with those of SOG, but to a slightly lower level than those of CSG-8W and CSG-12W. On the other hand, the increased trends of the gremlin-1 level observed in the lungs of CSG-8W and CSG-12W significantly decreased in CSG-CLS (Figure 2A through 2E and Figure S2). Together, these results indicated an overall recovery of systemic-to-pulmonary shunt induced BMP cascade suppression and gremlin-1 expression increment after cervical shunt ligation in rats of CSG-CSL.

Systemic-to-Pulmonary Shunt Increased Plasma Gremlin-1 Level Over Time in Rats

Interestingly, systemic-to-pulmonary shunt time-dependently induced a prominent increase of plasma gremlin-1 level in rats, whereas systemic-to-pulmonary shunt elimination terminated this trend (Figure 2F). Furthermore, plasma gremlin-1 concentration in SOG, CSG-8W, CSG-12W, and CSG-CSL revealed a close correlation with right ventricular systolic pressure, right ventricular developed pressure, the positive and negative maximum of right ventricular pressure, pulmonary arterial systolic pressure, mPAP, pulmonary arterial systolic pressure/systolic blood pressure, mPAP/mean systemic blood pressure, and ratio of the wet weight of right ventricle/that of the left ventricle plus septum (Figure 2G through 2P), theoretically indicating the potential of secretary gremlin-1 to be used as a new biomarker for patients with CHD-PAH.

Immunofluorescence staining demonstrated that gremlin-1, colocalized with von Willebrand factor (an endothelium biomarker), was mainly expressed in the endothelial layer of PAs (25–75 μm IED) in lungs from SOG and CSG-8W (Figure 2Q). Gremlin-1 colocalized with smooth muscle α-actin (a smooth muscle marker) was not found in the medium of PAs (25–75 μm IED) in lungs from SOG, but an intense expression of gremlin-1 colocalized with smooth muscle α-actin was detected in the medium of PAs (25–75 μm IED) with prominent medial hypertrophy and in PAs (<25 μm IED) with pervasive recurrence of smooth muscle layer in lungs from CSG-8W (Figure 2R), thus indicating that systemic-to-pulmonary shunts induced gremlin-1 expression increase in the medial layer of remodeled PAs.

Mechanical Stretch Stimulated Gremlin-1 Expression and Suppressed BMP Cascade in dPASMCs From Healthy Rats

Compared with the level of statically cultured dPASMCs, mechanical stretch (15%, 1 Hz) time-dependently promoted gremlin-1 mRNA level, but suppressed BMPR2 and Id1 mRNA levels (Figure 3A through 3C), whereas mechanical stretch (24 hours,

Figure 2. Expression change of BMP (bone morphogenetic protein) cascade and gremlin-1 in rats with persistent systemic-to-pulmonary shunt or cervical shunt ligation.

A, Representative Western blotting image of gremlin-1, BMP cascade (BMP receptor 2 [BMPR2], P-Smad1/5/8 [phosphorylated drosophila mothers against decapentaplegic protein 1/5/8], T-Smad1/5/8 [total drosophila mothers against decapentaplegic protein 1/5/8], and inhibitor of DNA-binding 1 [Id1]) in lungs from sham operation group (SOG) and combined surgery group (CSG). **B** through **D**, Quantitative analysis of BMP cascade by densitometric scanning: BMPR2 (**B**), P-Smad1/5/8 (**C**), and Id1 (**D**). **E**, Protein level of gremlin-1 in lungs from SOG and CSG. **F**, Plasma gremlin-1 concentration presented a stepwise increase in a time-dependent manner and decreased after cervical shunt closure. **G** through **P**, Regression scatterplot results demonstrate the correlation between plasma gremlin-1 level and right ventricular systolic pressure (RVSP) (**G**), right ventricular developed pressure (RVDP) (**H**), positive maximum RV dP/dt (+RV dp/dtmax) (**I**), negative maximum RV dP/dt (–RV dp/dtmax) (**J**), pulmonary arterial systolic pressure (PASP) (**K**), pulmonary artery diastolic pressure (PADP) (**L**), mean pulmonary arterial pressure (mPAP) (**M**), ratio of pulmonary arterial systolic pressure/systemic arterial systolic pressure (Pp/Ps) (**N**), mPAP/mean systemic blood pressure (mSBP) (**O**), and ratio of the weight of right ventricle/that of left ventricle plus septum (RV/LV+S) (**P**). **Q**, Immunofluorescence for gremlin-1 (green), von Willebrand factor (vWF; red), and nuclei (blue) in lung sections from SOG and CSG reserving for 12 weeks (CSG-12W) (bar=25 μm). White arrow indicates the colocalization of gremlin-1 with vWF. **R**, Immunofluorescence for gremlin-1 (green), smooth muscle α-actin (α-SMA) (red), and nuclei (blue) in lung sections from SOG and CSG-12W (bar=25 μm). White arrow indicates the colocalization of gremlin-1 with α-SMA. Data are mean±SD. n=9 to 10 rats per group. CSG-8W indicates CSG reserving for 8 weeks; CSG-CSL, CSG receiving cervical shunt ligation at the postoperative eighth week and continuously kept for the subsequent 4 weeks; DAPI, 4′6-diamidino-2-phenylindole; and NS, not significant. **P*<0.05, ***P*<0.01, and NS *P*>0.05.

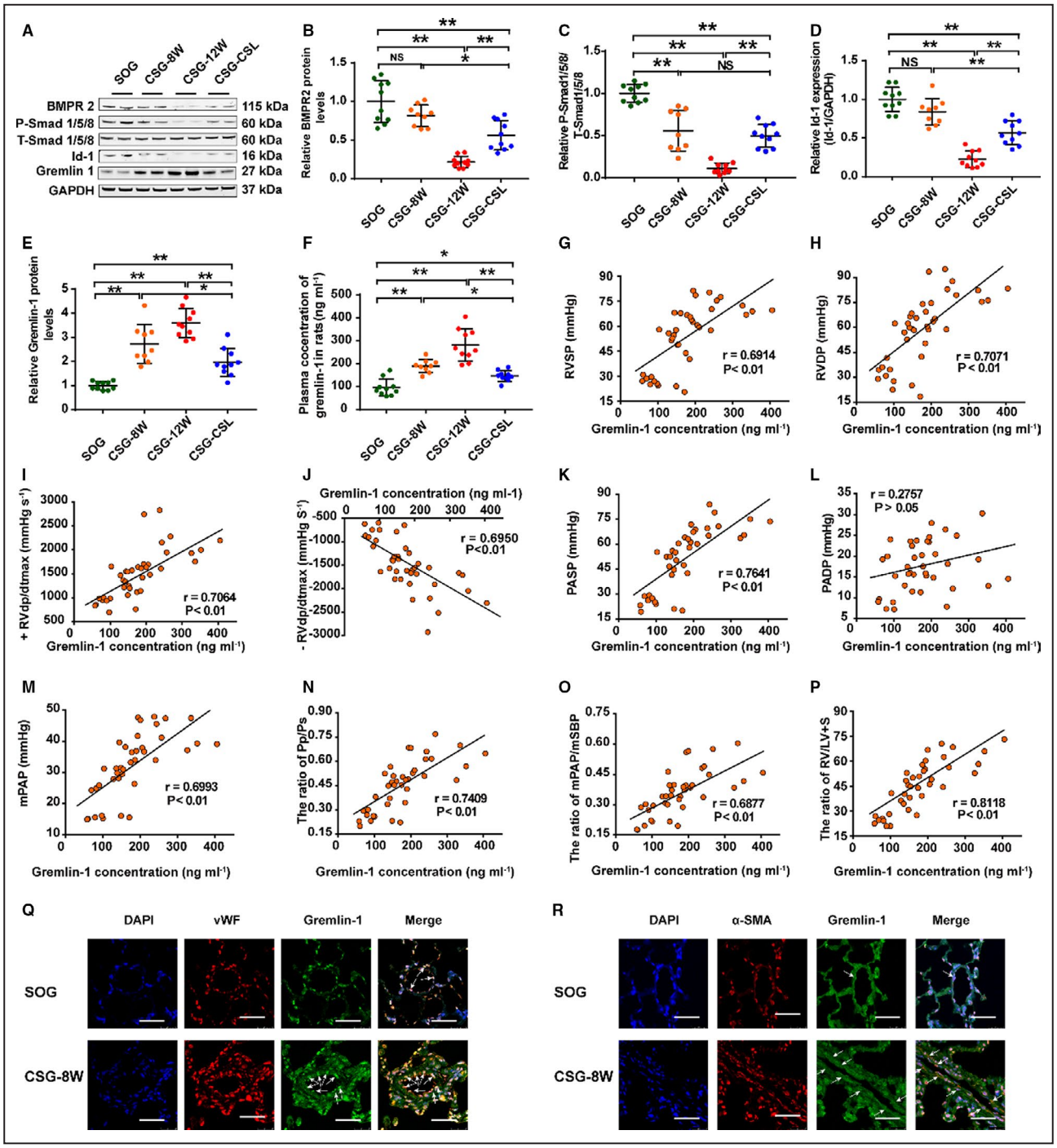

1 Hz) amplitude-dependently upregulated the mRNA level of gremlin-1, yet down-regulated the mRNA level of BMPR2 and Id1 (Figure 3D through 3F). Furthermore, mechanical stretch (15%, 24 hours, and 1 Hz) induced upregulation of gremlin-1 protein level and corresponding down-regulation of BMPR2, Smad1/5/8 phosphorylation, and Id1 expression in dPASMCs (Figure 3G through 3K), as shown by Western blotting, which suggested a significant suppression of BMP cascade in dPASMCs exposed to mechanical stretch (15%, 24 hours, and 1 Hz).

Effects of Gremlin-1 on dPASMCs From Healthy Rats Under Static Condition

Gremlin-1 Expression Was Upregulated in Proliferative dPASMCs

To further examine the expression pattern of gremlin-1 under static condition, dPASMCs were first synchronized with 0.4% fetal bovine serum and then recovered in complete smooth muscle cell medium for 0, 12, and 24 hours. At 0 hours, most cells were in the G0/G1 phase of the cell cycle, whereas at 12 and 24 hours,

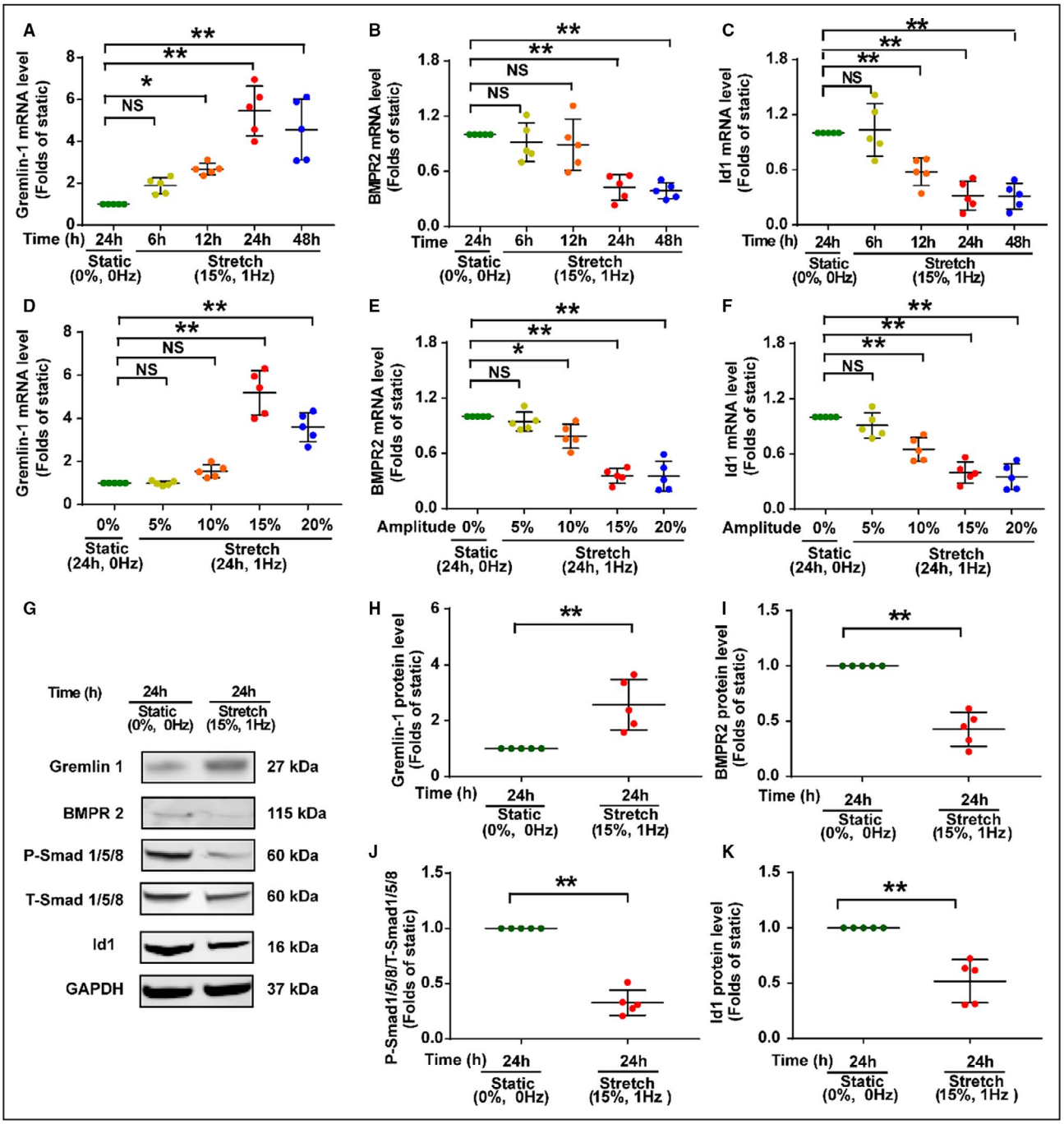

Figure 3. Mechanical stretch increased gremlin-1 expression and suppressed BMP (bone morphogenetic protein) cascade in distal pulmonary arterial smooth muscle cells (dPASMCs) from healthy rats.

A through **C**, Mechanical stretch (24 hours, 1 Hz) increased the mRNA level of gremlin-1 (**A**) but decreased the mRNA level of BMP receptor 2 (BMPR2) (**B**) and inhibitor of DNA-binding 1 (Id1) (**C**) in an amplitude-dependent way and achieved the optimal effect at 15%. **D** through **F**, Mechanical stretch (15%, 1 Hz) increased the mRNA level of gremlin-1 (**D**) but decreased the mRNA level of BMPR2 (**E**) and Id1 (**F**) in a time-dependent manner and exerted an optimal effect at 24 hours. **G**, Representative Western blotting image showing that the protein level changes of gremlin-1 and BMP cascade in dPASMCs under the condition of mechanical stretch (15%, 24 hours, and 1 Hz). **H** through **K**, Quantification analysis presented the protein level change of gremlin-1 (**H**), BMPR2 (**I**), P-Smad1/5/8 ([phosphorylated drosophila mothers against decapentaplegic protein 1/5/8) (**J**), and Id1 (**K**) in dPASMCs under the condition of mechanical stretch (15%, 24 hours, and 1 Hz). Data are mean±SD of 5 to 6 independent experiments. NS indicates not significant; and T-Smad1/5/7, total drosophila mothers against decapentaplegic protein 1/5/8. *P<0.05, **P<0.01, and NS P>0.05.

cells in S and G2/M phase gradually increased (Figure 4A). Compared with those of dPASMCs at 0 hours, apparent increases of gremlin-1 mRNA and protein level were observed (Figure 4B through 4C). Interestingly, proliferative dPASMCs correspondingly secreted gremlin-1 into the culture supernatant in a similar manner (Figure 4D).

Gremlin-1 Promoted the Proliferation of dPASMCs

As demonstrated in Figure 4E and Figure S3A, recombinant BMP2 and BMP4 dose-dependently inhibited dPASMC proliferation, achieving optimally inhibitory effect at 20 ng/mL. Interestingly, when simultaneously added with BMP2/4 (20 ng/mL), gradient gremlin-1 commenced restoring dPASMC proliferation at 10 ng/mL and procured an optimally reversal effect on dPASMC proliferation at 100 ng/mL for BMP2, whereas gradient gremlin-1 protein started restoring dPASMC proliferation at 100 ng/mL and procured an optimally reversal effect on dPASMC proliferation for BMP4 at 1000 ng/mL (Figure 4F and Figure S3B). Furthermore, anti–gremlin-1 (5 μg/mL)+BMP2 (20 ng/mL)+gremlin-1 (100 ng/mL) suppressed the proliferative capacity of dPASMCs to 76.25% of that of BMP2 (20 ng/mL)+gremlin-1 (100 ng/mL) group, whereas anti–gremlin-1 (15 μg/mL)+BMP4 (20 ng/

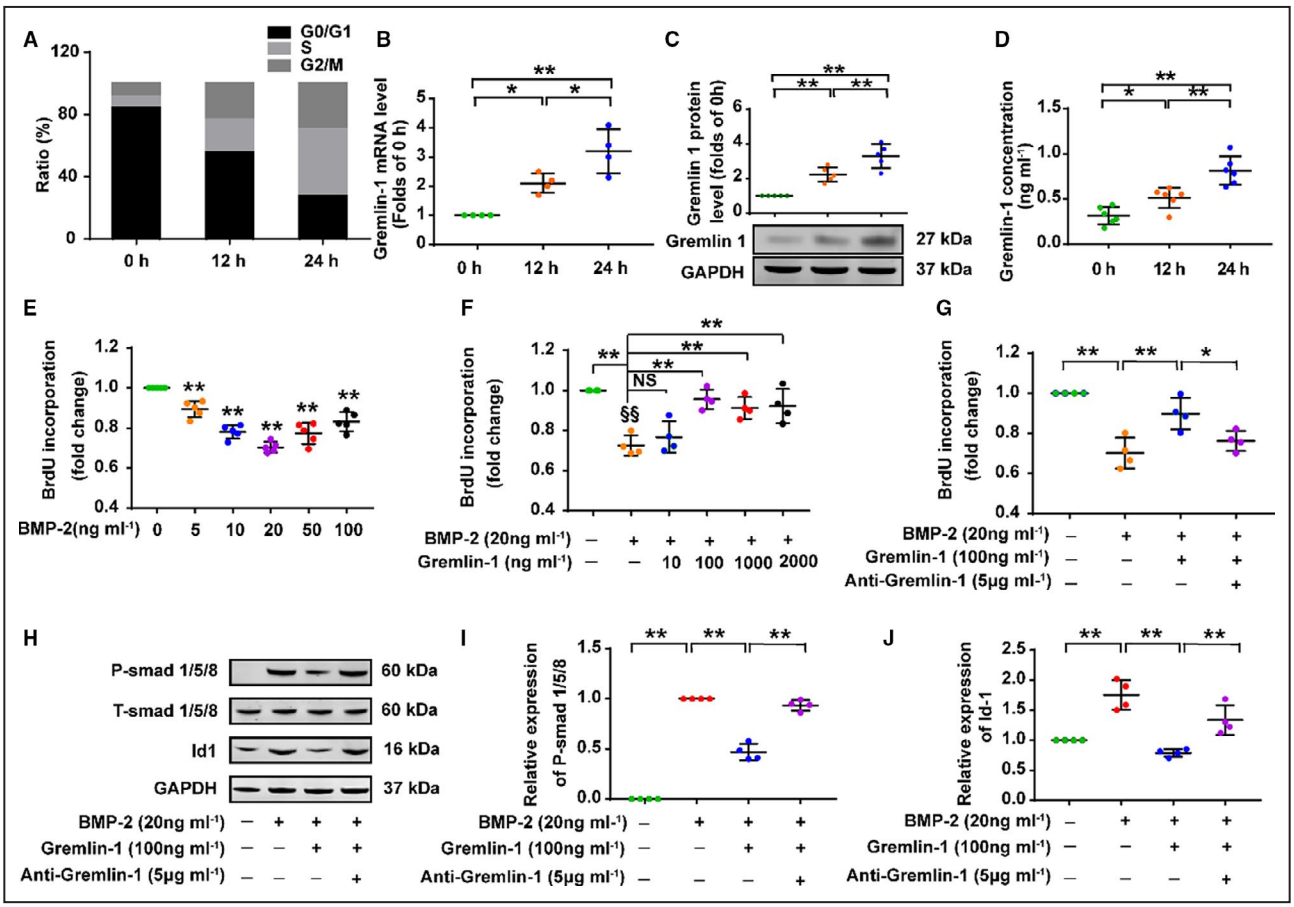

Figure 4. Gremlin-1 antagonized the inhibitory effect of BMP2 (bone morphogenetic protein 2) on distal pulmonary arterial smooth muscle cell (dPASMC) proliferation.

A, Quantitative analysis of dPASMC distribution in cell phase at indicated time point. **B**, mRNA expression of gremlin-1 in dPASMCs after recovery in CSMCM for 0, 12, and 24 hours. **C**, Representative Western blotting image (lower panel) and densitometric analysis (upper panel) showing the protein level change of gremlin-1 in dPASMCs after recovery in CSMCM for 0, 12, and 24 hours. **D**, The concentration of gremlin-1 secreted into culture medium, as detected by ELISA. **E**, BMP2 dose-dependently suppressed dPASMC proliferation and procured the maximal inhibitory effect at 20 ng/mL. **F**, Gremlin-1 dose-dependently antagonized the proliferation suppressive effect of BMP2 (20 ng/mL) on dPASMCs and reached the maximally antagonistic effect at 100 ng/mL. **G**, Anti–gremlin-1 (5 μg/mL) reversed the maximally antagonistic effect of gremlin-1 (100 ng/mL) for BMP2 (20 ng/mL). **H** through **J**, Representative Western blotting image and densitometric analysis showing that BMP2 at 20 ng/mL induced significant Smad1/5/8 (drosophila mothers against decapentaplegic protein 1/5/8) phosphorylation (**H** and **I**) and inhibitor of DNA-binding 1 (Id1) expression activation (**H** and **J**) in dPASMCs, which was apparently antagonized by gremlin-1 at 100 ng/mL and reversed by additional anti–gremlin-1 at 5 μg/mL. Data are mean±SD of 4 to 5 independent experiments. BrdU indicates 5-bromo-2-deoxy-uridine; CSMCM, complete smooth muscle cell medium; and NS, not significant. **P*<0.05, ***P*<0.01, and NS *P*>0.05.

mL)+gremlin-1 (1000 ng/mL) suppressed the proliferative capacity of dPASMCs to 75.38% of that of BMP4 (20 ng/mL)+gremlin-1 (1000 ng/mL) group (Figure 4G and Figure S3C).

Under the static culture condition (Figure 4H through 4J and Figure S3D through S3F), recombinant BMP2/4 (20 ng/mL) significantly upregulated Smad1/5/8 phosphorylation and Id1 expression in dPASMCs compared with control group, whereas gremlin-1 (100 ng/mL for BMP2, 1000 ng/mL for BMP4) coincubated with dPASMCs significantly antagonized BMP2/4 (20 ng/mL) and induced Smad1/5/8 phosphorylation and Id1 expression. Furthermore, addition of anti–gremlin-1 (5 μg/mL for gremlin-1 of 100 ng/mL, 15 μg/mL for gremlin-1 of 1000 ng/mL) apparently blocked the antagonizing effect of gremlin-1 on BMP2/4 incurring expression level of Smad1/5/8 phosphorylation and Id1 transcription.

Gremlin-1 Inhibited the Apoptosis of dPASMCs

As shown in Figure 5A and 5B and Figure S4A and S4B, under the baseline culture condition, the apoptotic rate ranged from 13.53±4.10% in control dPASMCs. Treatment of dPASMCs with recombinant gremlin-1 alone in incremental gradient (0, 1, 10, 100, and 1000 ng/mL) had no effect on dPASMC apoptosis (data not shown); however, treatment of dPASMCs with BMP2/4 at 20 ng/mL for 24 hours significantly increased the percentage of apoptotic dPASMCs. Interestingly, when cotreated with BMP2 (20 ng/mL)+gremlin-1 (100 ng/mL) or BMP4 (20 ng/mL)+gremlin-1 (1000 ng/mL), the percentage of dPASMC apoptosis furthermore decreased, whereas anti–gremlin-1 (5 μg/mL for gremlin-1 of 100 ng/mL, 15 μg/mL for gremlin-1 of 1000 ng/mL) reversed the apoptosis rate to a similar level observed in dPASMCs only exposed to BMP2/4 (20 ng/mL), thus indicating that gremlin-1 exerted an antiapoptotic effect on dPASMCs via BMP cascade.

Simultaneously, as presented in Figure 5C through 5F and Figure S4C through S4F, incubation of dPASMCs with BMP-2/4 (20 ng/mL) for 24 hours significantly downregulated the expression level of Bcl-2, but coincubation of dPASMCs with BMP2 (20 ng/mL)+gremlin-1 (100 ng/mL) or BMP4 (20 ng/mL)+gremlin-1 (1000 ng/mL) for 24 hours reversed this decreasing trend of Bcl-2 level to a slight lower level than those of control dPASMCs, whereas anti–gremlin-1 (5 μg/mL for BMP2+gremlin-1, 15 μg/mL for

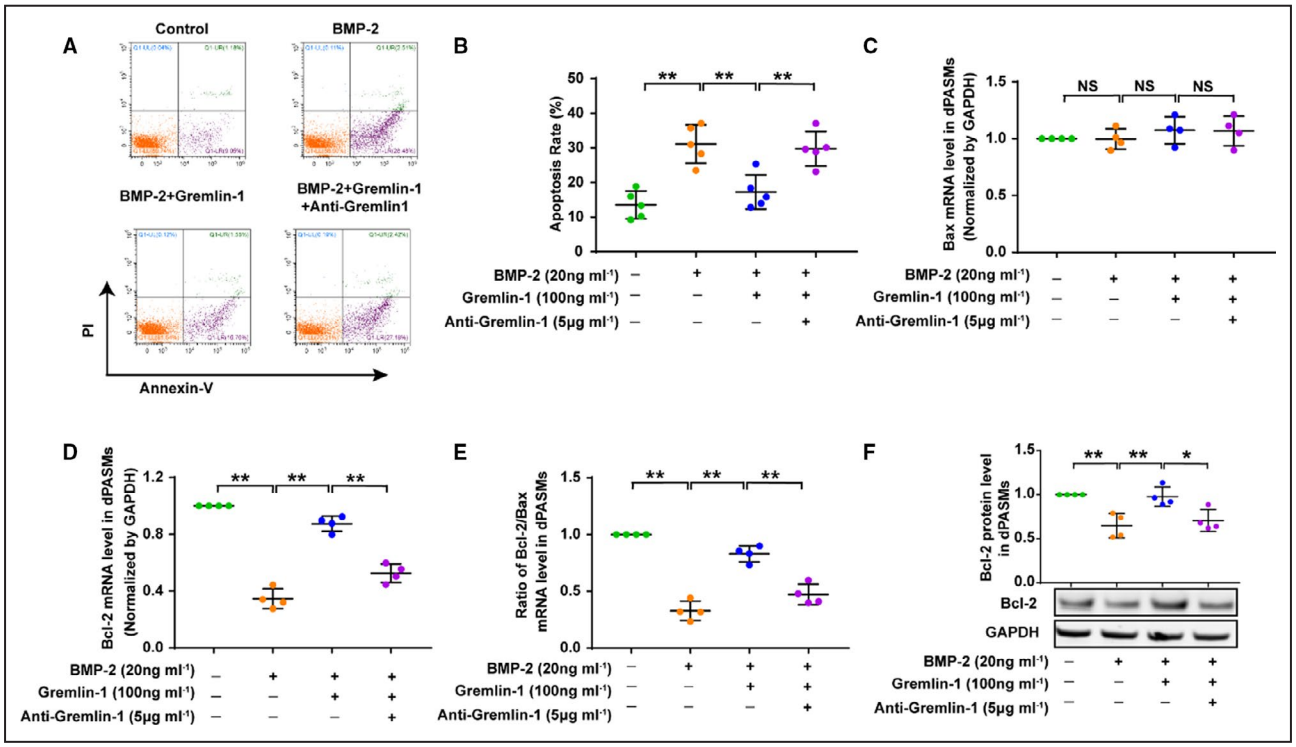

Figure 5. Gremlin-1 blocks the proapoptotic effects of BMP2 (bone morphogenetic protein 2) on distal pulmonary arterial smooth muscle cells (dPASMCs).

A, Representative flow cytometry images showing the effects of BMP2, BMP2+gremlin-1, and BMP2+gremlin-1+anti–gremlin-1 on the apoptosis of dPASMCs. **B**, Quantification of apoptotic cells. **C** through **F**, Effect of BMP2, BMP2+gremlin-1, and BMP2+gremlin-1+anti–gremlin-1 on Bax mRNA level (**C**), B-cell lymphoma-2 (Bcl-2) mRNA level (**D**), ratio of Bcl-2/Bax (**E**), and Bcl-2 protein level (**F**) in dPASMCs. Data are mean±SD of 4 to 5 independent experiments. NS indicates not significant. **P*<0.05, ***P*<0.01, and NS *P*>0.05 vs control group.

BMP4+gremlin-1) decreased the expression level of Bcl-2 down to a similar level observed in dPASMCs exposed to BMP2/4 (2 0 ng/mL). Negligible effect of BMP2/4, BMP2/4+gremlin-1, and BMP2/4+gremlin-1+anti–gremlin-1 was observed, on the mRNA expression of Bax, so the ratio of Bcl-2/Bax mRNA levels (Bcl-2/Bax) also demonstrated a similar trend with Bcl-2.

Gremlin-1 Increased in Patients With CHD-PAH

Gremlin-1 Expression Increased in Explanted Lung Tissues From Patients With End-Stage CHD-PAH

As demonstrated in Figure 6, when compared with control subjects, the mRNA and protein expression levels of gremlin-1 in lungs from patients with Eisenmenger syndrome were significantly upregulated. Furthermore, immunohistochemical staining revealed that gremlin-1 was predominantly localized in endothelium but not detectable in medium and adventitia in distal pulmonary arteries of control lungs. Interestingly, gremlin-1 staining was further enhanced in endothelium and markedly expressed in medium, but still not detectable in adventitia of remodeled distal pulmonary arteries (Figure 6C), which, in turn, indicated that systemic-to-pulmonary shunt induced the enhancement of gremlin-1 staining in endothelium and emergence in the medium of resistant distal pulmonary arteries.

Plasma Concentration of Gremlin-1 Indicated the Extent of CHD-PAH

Compared with age- and sex-matched control subjects, a significant increase of circulating gremlin-1 accompanied the deterioration of CHD-PAH (Figure 6D). Furthermore, the plasma concentration of gremlin-1

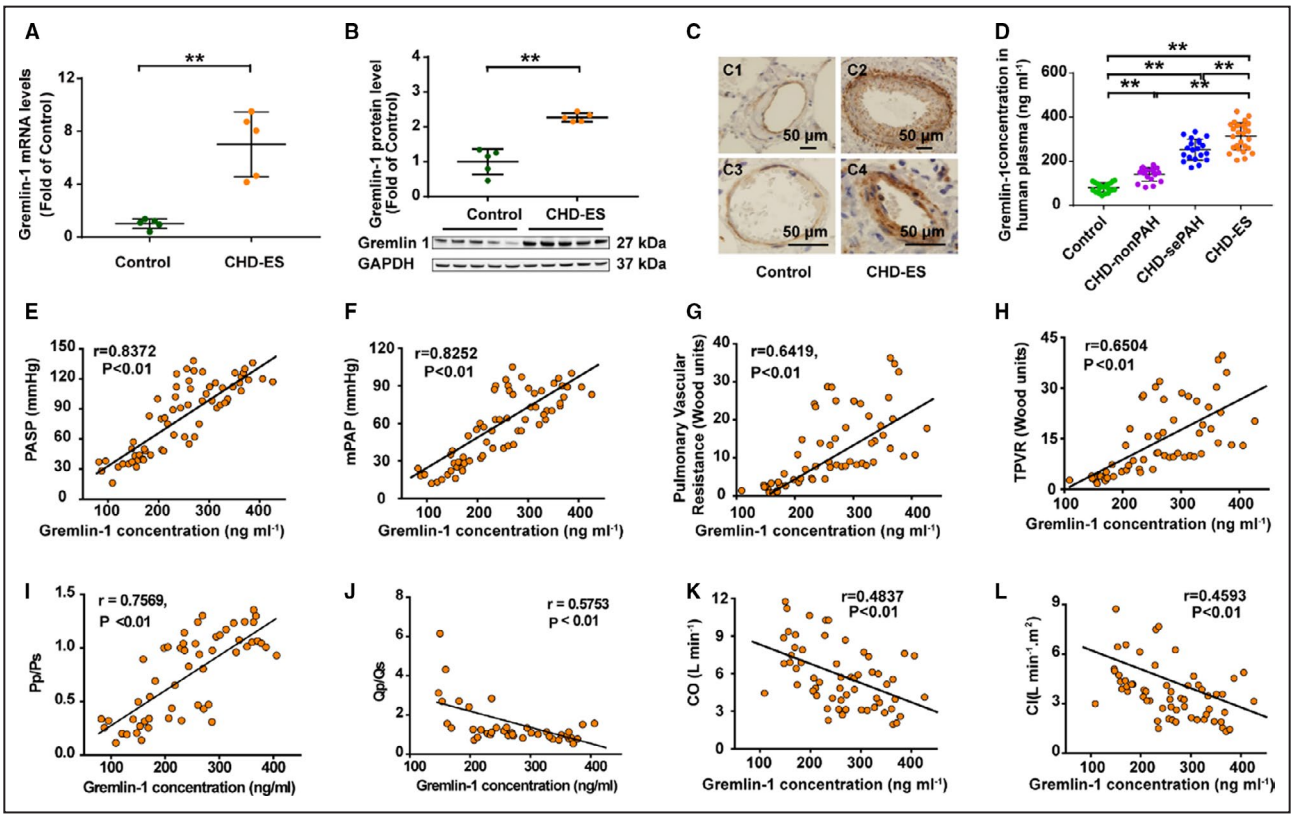

Figure 6. Gremlin-1 expression increased in patients with congenital heart disease with Eisenmenger syndrome (CHD-ES). **A**, mRNA level of gremlin-1 in patients with CHD-ES (n=5) and control subjects (n=5). **B**, Representative Western blotting image of gremlin-1 protein level (lower panel) and densitometric analysis (upper histogram) in patients with CHD-ES (n=5) and control subjects (n=5). **C**, Representative images of immunohistological staining of gremlin-1 in control lungs (C1 and C2, ×40) and lungs with CHD-ES (C3 and C4, ×100) (bar=50 μm). **D**, Plasma level of gremlin-1 demonstrated a stepwise increase with the extent of CHD-associated pulmonary arterial hypertension (CHD-PAH). **E** through **L**, Plasma level of gremlin-1 positively correlated with pulmonary arterial systolic pressure (PASP) (**E**), mean pulmonary arterial pressure (mPAP) (**F**), pulmonary vascular resistance (**G**), total pulmonary vascular resistance (TPVR) (**H**), and ratio of pulmonary arterial systolic pressure/systemic arterial systolic pressure (Pp/Ps) (**I**), and negatively correlated with pulmonary/systemic shunt volume ratio (Qp/Qs) (**J**), cardiac output (CO) (**K**), and cardiac index (CI) (**L**). sePAH indicates severe PAH. ***P*<0.01.

was closely correlated with pulmonary hemodynamic parameters (Figure 6E through 6L), which indicated that gremlin-1 might be used as a potential pathogenesis-linked biomarker for CHD-PAH.

DISCUSSION

PAH frequently encountered in patients with CHD represents a particular subtype among PAH clinical classifications based on pathologic, pathophysiological, and clinical therapeutic features.[15] Previous studies have confirmed that PAH subtypes share some common molecular and pathologic mechanisms, whereas CHD-PAH has some distinctive characteristics in cause and pathogenesis, such as initial impetus (systemic-to-pulmonary shunt), early-stage hyperoxia in pulmonary circulation for systemic-to-pulmonary shunt, end-stage hypoxia after reversal of systemic-to-pulmonary shunt, less of inflammation involvement, and rare pathogenic mutations.[1] Consequently, extrapolating parallel data from other PAH subtypes to the field of CHD-PAH needs to be done with a certain caution.

Gremlin-1 and BMP Signal Pathway

Gremlin-1 was initially discovered in a Xenopus embryo cDNA library with biologically dorsalizing activity for its antagonism of BMPs.[19] Previous developmental research found that gremlin-1 could be detected in embryonic lungs, and gremlin-1 overexpression or knockout resulted in the disruption of normal airway morphogenesis, lung vascular branching, defects in lung septation, or neonatal death.[20–22] Functional experiments found that gremlin-1 could be noncovalently anchored to cellular membrane or secreted into culture medium or blood, where it is capable of binding to BMPs, thus blocking their interaction with their cognate receptors and changing the effective concentration of its free or active form.[13,23,24] Among the characterized BMP family members, gremlin-1 specifically and preferentially binds to BMP-2/4, which have been studied in detail in PAH.[15,19,25] Under the physiological condition, BMPs have a crucial role in maintaining the homeostasis, integrity, and function of normal pulmonary circulation,[26,27] whereas genetic abnormalities in BMP receptor 2 (BMPR2) cause primary PAH,[28–30] indicating that the balance between gremlin-1 and BMPs is crucial in lung homeostasis. However, patients with CHD-PAH tend to present with rare BMPR2 mutation and common reduction of BMP signaling in lungs without reasonable explanation,[7,9] so gremlin-1 change in lungs exposed to systemic-to-pulmonary shunts and its antagonism of BMP cascade may provide a new mechanical explanation for this special PAH subtype.

Parallel Data on the Role of Gremlin-1 in Vascular Remodeling

Pathological property switch of vascular smooth muscle cells (VSMCs) from a “contractile” phenotype (a quiescent, nonmigratory, and differentiated state) to a “synthetic” phenotype (a proliferative, migratory, and apoptosis-resistant state) is the standard and central mechanism shared by systemic vascular remodeling and pulmonary vascular remodeling; thus, analogous evidence from systemic vascular remodeling and pulmonary vascular remodeling of other PAH subtypes may offer some insights in the field of pulmonary vascular remodeling of CHD-PAH.

In systemic vasculature, parallel research also found that gremlin-1 was constitutively expressed at a relatively weak level in rat VSMCs from systemic arteries (aorta or carotid), and was significantly upregulated in the neointima of rat carotid arteries following balloon injury, remaining detectable at the 28th day of injury. Furthermore, in vitro studies found that gremlin-1 markedly facilitated the proliferation and migration of VSMCs via BMP antagonism, indicating the promoting roles of gremlin-1 in systemic vascular remodeling.[15]

Interestingly, in adult lungs, previous studies reported that alveolar hypoxia significantly upregulated gremlin-1 expression, which was mainly ascribed to its selective activation in pulmonary arterial endothelial cells (PAECs). Sequential studies further confirmed that gremlin-1 gene knockout or blockage with neutralizing antibody partially attenuated the hypoxia or hypoxia/SU5416 induced mice PAH, yet it would be arbitrary to affirm that gremlin-1 exerts identical roles in CHD-PAH with those confirmed in hypoxia PAH. Systemic-to-pulmonary shunt–induced PAH is a special type of PAH, which is a different form, and even contrary to hypoxic PAH in some aspects. First, these 2 PAH subsets have different initial impetuses (ie, in hypoxic PAH, alveolar hypoxia first provokes alveolar epithelium, macrophages, and pulmonary adventitial fibroblasts, whereas in systemic-to-pulmonary shunt–induced PAH, flow and pressure overload in pulmonary circulation mainly first affect the PAECs and PASMCs via increased shear stress and intraluminal mechanical stretch). Second, pulmonary vasculopathy observed in hypoxia PAH is common of stage Ⅰ, according to Heath-Edwards classification, but of stage Ⅰ to Ⅲ in systemic-to-pulmonary shunt–induced PAH.[16,17] Third, patients with hypoxia PAH tend to experience progressively accelerated hypoxia throughout the disease, whereas patients with CHD-PAH are exposed to hyperoxia at the early stage when systemic-to-pulmonary shunt still exists and hypoxia at the end stage of CHD-PAH when reversal of systemic-to-pulmonary shunt emerges. Consequently, further validation experiment should

be performed on an acceptable shunt-related model to confirm the accurate distribution, change, and roles of gremlin-1 in response to systemic-to-pulmonary shunts. Furthermore, gremlin-1 expression was ≈8-fold higher in the lungs of patients with idiopathic PAH but no BMPR2 mutation.[31]

Given these parallel research results, we particularly focused on gremlin-1 in lungs exposed to systemic-to-pulmonary shunts, which may present a persuasive mechanism explanation for BMP signal reduction in lungs from patients with CHD-PAH but without heterozygous loss-of-function mutations in BMPR2.

Tissue and Cell Source of Gremlin-1

Existing studies have reported that gremlin-1 could be detected in pulmonary vascular endothelium, proximal airway epithelium, alveolar epithelium, fibroblasts, and macrophages,[20,31–33] which presented a similar cellular distribution with BMPR2 expression and Smad signaling.[34–39] However, up to now, no study has investigated the expression pattern of gremlin-1 in distal PASMCs and its biological roles in the phenotype change of distal PASMCs, especially under the condition of systemic-to-pulmonary shunts.

To the best of our knowledge, this is the first study that reported on systemic-to-pulmonary shunt inducing a persistent increase of gremlin-1 in lungs compared with those of normal lungs (Figure 2A and 2E), which is consistent with previous research on hypoxia PAH.[13,31] Sequential immunohistochemistry and immunofluorescence analysis performed in patients and rats demonstrated that in normal PAs, gremlin-1 was predominantly localized in the endothelium but undetectable in the medial layer or adventitia, whereas in severely remodeled PAs, intense gremlin-1 staining was observed in the neointima and medial layer but not alveolar macrophages (Figure 2Q and 2R). On the other hand, previous studies found that hypoxia enhanced gremlin-1 staining in PAECs and alveolar macrophages but not in medial PASMCs. These discrepancies of gremlin-1 distributions may be attributed to their disparities in the impetus and extent of these 2 PAH subtypes. In hypoxia PAH, pulmonary vasculopathy was mainly of stage Ⅰ lesion by Heath-Edwards classification and no neointima formation emerged,[31] which indicated that the proportion of phenotype changed PASMCs was relatively lower. In contrast, hypoxia confirmative activated alveolar macrophages.[40] Nevertheless, in shunted PAH, flow and pressure overload in pulmonary circulation increased intraluminal shear stress and mechanical stretch that inevitably initiated and advanced the phenotype change of PAECs and PASMCs. Therefore, pulmonary vasculopathy of stage Ⅰ to Ⅲ of Heath-Edwards classification was frequently observed,[16] which indicated the higher proportion of proliferative PAECs and PASMCs in remodeling pulmonary vascular wall. Nonetheless, no study confirmed that systemic-to-pulmonary shunt could activate alveolar macrophages. Moreover, data on human lungs also demonstrated no staining of gremlin-1 in PA media; however, these human lung specimens were all from patients with idiopathic or heritable PAH,[13,31] whereas no lung specimens from patients with Eisenmenger syndrome were used. Taken together, we could conclude that gremlin-1 expression is diverse in PAH of different subtypes or divergent cell types.

Stimuli of Gremlin-1 Expression or Secretion

In systemic vasculature, gremlin-1 is constitutively expressed in VSMCs of rat aorta and carotid, and intraluminally mechanical injury or growth factors (transformed growth factor-β1, platelet-derived growth factor, and angiotensin Ⅱ) could significantly upregulate gremlin-1 expression,[15] whereas in the pulmonary vasculature, hypoxia (10% O_2 for 48 hours) could selectively activate gremlin-1 gene expression in murine lungs and stimulated gremlin-1 protein secretion from human PAECs in vitro. Furthermore, treatment with gremlin-1 neutralizing antibody demonstrated prophylactic and therapeutic effects in hypoxic/SU5416-induced pulmonary vascular remodeling and right ventricular hypertrophy. Interestingly, no attention was focused on PASMCs in these in vivo serial studies, which may be misdirected by the observation that no staining of gremlin-1 was found in the media of PAs of hypoxia PAH, or assumption that gremlin-1 may not participate in the biological behavior of PASMCs exposed to hypoxia.[15,20,33] Although this study further confirmed that systemic-to-pulmonary shunt induced increase of gremlin-1 expression in rat lungs, and the increased gremlin-1 was mainly localized in the neointima and media of remodeled PAs, subsequent in vitro experiments found that mechanical stretch time- and amplitude-dependently stimulated gremlin-1 expression and suppressed BMP signaling pathway in distal PASMCs from healthy rats (Figure 3), which, in turn, indicated the pathogenic involvement of gremlin-1 in the genesis and progression of CHD-PAH.

Gremlin-1 Promoted the Phenotype Changes of dPASMCs

Previous studies have reported that gremlin-1 is wildly expressed in various tumor or hyperplasia tissues, such as lung, breast, digestive system (esophagus,

pancreas, and colon), reproductive system (ovary, cervix, and endometrium), urinary system (kidney, prostate, and bladder), mesothelioma, and synoviocyte hyperplasia.[41–43] Further functional studies found that gremlin-1 knockdown significantly inhibited the proliferation, migration, and invasion of tumor cells in a BMP-dependent or BMP-independent way, but promoted apoptosis through the accumulation of Bax, cleaved caspase-3, and downregulation of Bcl-2, whereas gremlin-1 overexpression BMP-independently induced tumor cell proliferation, migration, and invasion.[44,45] Research on vascular components revealed that hypoxia (1% O_2, 24 hours) elicited gremlin-1 stimulated the proliferation and migration of human PAECs in a Nox1/Ref-1-CREB-dependent manner.[46] Interestingly, Maciel et al found that gremlin overexpression accelerated the proliferation and migration of VSMCs through $p27^{kip1}$ downregulation.[15] In contrast, gremlin gene silencing promoted a significant blockade on VSMC proliferation and migration. In clonal rat embryonic VSMCs, gremlin overexpression increased apoptosis, as demonstrated by chromatin morphological features and caspase-3 activity, whereas gremlin gene silencing effectively suppressed apoptosis in clonal rat embryonic VSMCs and rabbit VSMCs. Consequently, they concluded that gremlin promotes the proliferation, migration, and apoptosis of VSMCs.[15,47] This existing evidence showed that gremlin-1 could affect diverse cellular functions, including growth, differentiation, and development, whereas in the present study, we found that in vivo mechanical stretch stimulated the secretion of gremlin-1 from distal PASMCs and gremlin-1 promoted the proliferation but inhibited the apoptosis of dPASMCs (Figures 3 through 5), which corresponds to the central feature of pulmonary vascular remodeling (ie, phenotype alteration of PASMCs [from a quiescent, nonmigratory, and differentiated state to a proliferation, migration, and synthetic state]).[2]

Gremlin-1 Represented an Underlying Mechanical Biomarker for CHD-PAH

Interestingly, Wellbrock et al reported that plasma gremlin-1 levels elevated in patients with PAH were inversely correlated with patients' functional status and significantly stratified the overall survival of patients with PAH; thus, they considered that gremlin-1 was a potential biomarker for PAH that was directly associated with the underlying mechanism.[48] However, the number of specimens in their study was only 31, and the types of PAH were diverse, including hereditary, idiopathic, and secondary PAH. Also, some clinical data were not available, so it is only an investigative trial with limited clinical guiding significance. In the present study, only patients with CHD-PAH were included, the number of patients was much larger, and the baseline information and detailed clinical data, including right heart hemodynamic parameters, were available. Our results not only demonstrated a similar trend, as reported by Wellbrock et al,[48] but also corroborated their findings, thus providing much more clinical guiding significance for the diagnosis and follow-up in patients with CHD-PAH. Nonetheless, large, multicentered prospective studies should be performed to determine the potential of gremlin-1 as a promising biomarker in clinical settings.

CONCLUSIONS

This is the first study that confirmed that systemic-to-pulmonary shunt incurred strong expression of gremlin-1 in the lungs, which was predominantly localized in PAECs and PASMCs of remodeled PAs. Furthermore, mechanical stretch upregulated gremlin-1 expression in distal PASMCs, which exerts promoting roles in dPASMC phenotype transformation partially mediated by BMP cascades, and increased plasma gremlin-1 was positively correlated with pulmonary hemodynamic indexes. These results implicated the potential of gremlin-1 to be a new biomarker and a therapeutic target for patients with CHD-PAH.

ARTICLE INFORMATION

Received April 20, 2020; accepted June 30, 2020.

Affiliations

From the State Key Laboratory of Cardiovascular Disease, Fuwai Hospital, National Center for Cardiovascular Disease, Chinese Academy of Medical Sciences and Peking Union Medical College (L.M., X.T., Y.L., J.M.), Medical Research Center, Beijing Chao-Yang Hospital, Capital Medical University, Beijing, China (W.Y., X.L.); Department of Rheumatology and Immunology, Jiangxi Provincial People's Hospital Affiliated to Nanchang University, Nanchang, Jiangxi, China (L.D.); Department of Organ Transplantation and Thoracic Surgery, The First Affiliated Hospital of Guangzhou Medical University, Guangzhou, China (C.Y.); Department of Cardiovascular Surgery Center, Beijing Anzhen Hospital, Capital Medical University, Beijing Institute of Heart, Lung and Blood Vascular Diseases, Beijing, China (S.W.); and Heart Center and Beijing Key Laboratory of Hypertension Research, Beijing Chao-Yang Hospital, Capital Medical University, Beijing, China (H.C., X.L.).

Sources of Funding

This work was supported by research grants from the Beijing Natural Science Foundation (grants 7172182 and 7172078), National Natural Science Foundation (grants 81400034, 81470424, 81500038, 81671544, and 81871286), Beijing Key Laboratory of Hypertension Research Open Foundation (grant 2019GXY-KFKT-02), and Capital Medical University Research and Development Fund (Nature) (grant PYZ19017).

Disclosures

None.

Supplementary Materials

Figures S1–S4

REFERENCES

1. Simonneau G, Gatzoulis MA, Adatia I, Celermajer D, Denton C, Ghofrani A, Sanchez MAG, Kumar RK, Landzberg M, Machado RF, et al.

Updated clinical classification of pulmonary hypertension. *J Am Coll Cardiol*. 2013;62:D34–D41.
2. Taisic T, Morrell NW. Smooth muscle cell hypertrophy, proliferation, migration and apoptosis in pulmonary hypertension. *Compr Physiol*. 2011;1:295–317.
3. Davies RJ, Morrell NW. Molecular mechanisms of pulmonary arterial hypertension: role of mutations in the bone morphogenetic protein type II receptor. *Chest*. 2008;134:1271–1277.
4. Machado RD, Pauciulo MW, Thomson JR, Lane KB, Morgan NV, Wheeler L, Phillips JA III, Newman J, Williams D, Galiè N, et al. BMPR2 haploinsufficiency as the inherited molecular mechanism for primary pulmonary hypertension. *Am J Hum Genet*. 2001;68:92–102.
5. Nasim MT, Ogo T, Chowdhury HM, Zhao L, Chen CN, Rhodes C, Trembath RC. BMPR-II deficiency elicits pro-proliferative and anti-apoptotic responses through the activation of TGFβ-TAK1-MAPK pathways in PAH. *Hum Mol Genet*. 2012;21:2548–2558.
6. Limsuwan A, Choubtum L, Wattanasirichaigoon D. 5'UTR repeat polymorphisms of the BMPR2 gene in children with pulmonary hypertension associated with congenital heart disease. *Heart Lung Circ*. 2013;22:204–210.
7. Roberts KE, McElroy JJ, Wong WP, Yen E, Widlitz A, Barst RJ, Knowles JA, Morse JH. BMPR2 mutations in pulmonary arterial hypertension with congenital heart disease. *Eur Respir J*. 2004;24:371–374.
8. Liu D, Liu QQ, Guan LH, Jiang X, Zhou DX, Beghetti M, Qu JM, Jing ZC. BMPR2 mutation is a potential predisposing genetic risk factor for congenital heart disease associated pulmonary vascular disease. *Int J Cardiol*. 2016;211:132–136.
9. Du L, Sullivan CC, Chu D, Cho AJ, Kido M, Wolf PL, Yuan JX, Deutsch R, Jamieson SW, Thistlethwaite PA. Signaling molecules in nonfamilial pulmonary hypertension. *N Engl J Med*. 2003;348:500–509.
10. Meng L, Liu X, Teng X, Yuan W, Duan L, Meng J, Li J, Zheng Z, Wei Y, Hu S. DAN plays important compensatory roles in systemic-to-pulmonary shunt associated pulmonary arterial hypertension. *Acta Physiol (Oxf)*. 2019;226:e13263.
11. Rondelet B, Kerbaul F, Van Beneden R, Motte S, Fesler P, Hubloue I, Remmelink M, Brimioulle S, Salmon I, Ketelslegers JM, et al. Signaling molecules in overcirculation-induced pulmonary hypertension in piglets: effects of sidenafil therapy. *Circulation*. 2004;110:2220–2225.
12. Rondelet B, Kerbaul F, Van Beneden R, Hubloue I, Huez S, Fesler P, Remmelink M, Brimioulle S, Salmon I, Naeije R. Prevention of pulmonary vascular remodeling and of decreased BMPR-2 expression by losartan therapy in shunt-induced pulmonary hypertension. *Am J Physiol Heart Circ Physiol*. 2005;289:H2319–H2324.
13. Cahill E, Costello CM, Rowan SC, Harkin S, Howell K, Leonard MO, Southwood M, Cummins EP, Fitzpatrick SF, Taylor CT, et al. Gremlin plays a key role in the pathogenesis of pulmonary hypertension. *Circulation*. 2012;125:920–930.
14. Ciuclan L, Sheppard K, Dong L, Sutton D, Duggan N, Hussey M, Simmons J, Morrell NW, Jarai G, Edwards M, et al. Treatment with anti gremlin 1 antibody ameliorates chronic hypoxia/SU5416-induced pulmonary arterial hypertension in mice. *Am J Pathol*. 2013;183:1461–1473.
15. Maciel TT, Melo RS, Schor N, Campos AH. Gremlin promotes vascular smooth muscle cell proliferation and migration. *J Mol Cell Cardiol*. 2008;44:370–379.
16. Meng L, Liu X, Zheng Z, Li J, Meng J, Wei Y, Hu S. Original rat model of high kinetic unilateral pulmonary hypertension surgically induced by combined surgery. *J Thorac Cardiovasc Surg*. 2013;146:1220–1226.
17. Heath D, Edwards JE. The pathology of hypertensive pulmonary vascular disease; a description of six grades of structural changes in the pulmonary arteries with special reference to congenital cardiac septal defects. *Circulation*. 1958;18:533–547.
18. Wagenvoort CA. Open lung biopsies in congenital heart disease for evaluation of pulmonary vascular disease: predictive value with regard to corrective operability. *Histopathology*. 1985;9:417–436.
19. Hsu DR, Economides AN, Wang X, Eimon PM, Harland RM. The Xenopus dorsalizing factor Gremlin identifies a novel family of secreted proteins that antagonize BMP activities. *Mol Cell*. 1998;1:673–683.
20. Lu MM, Yang H, Zhang L, Shu W, Blair DG, Morrisey EE. The bone morphogenic protein antagonist gremlin regulates proximal-distal patterning of the lung. *Dev Dyn*. 2001;222:667–680.
21. Shi W, Zhao J, Anderson KD, Warburton D. Gremlin negatively modulates BMP-4 induction of embryonic mouse lung branching morphogenesis. *Am J Physiol Lung Cell Mol Physiol*. 2001;280:L1030–L1039.
22. Michos O, Panman L, Vintersten K, Beier K, Zeller R, Zuniga A. Gremlin-mediated BMP antagonism induces the epithelial-mesenchymal feedback signaling controlling metanephric kidney and limb organo-genesis. *Development*. 2004;131:3401–3410.
23. Topol LZ, Bardot B, Zhang Q, Resau J, Huillard E, Marx M, Calothy G, Blair DG. Biosynthesis, post-translation modification, and functional characterization of Drm/Gremlin. *J Biol Chem*. 2000;275:8785–8793.
24. Gazzerro E, Canalis E. Bone morphogenetic proteins and their antagonists. *Rev Endocr Metab Disord*. 2006;7:51–65.
25. Church RH, Krishnakumar A, Urbanek A, Geschwindner S, Meneely J, Bianchi A, Basta B. Gremlin1 preferentially binds to bone morphogenetic protein-2 (BMP-2) and BMP-4 over BMP-7. *Biochem J*. 2015;466:55–68.
26. Morrell NW, Yang X, Upton PD, Jourdan KB, Morgan N, Sheares KK, Trembath RC. Altered growth responses of pulmonary artery smooth muscle cells from patients with primary pulmonary hypertension to transforming growth factor-beta(1) and bone morphogenetic proteins. *Circulation*. 2001;104:790–795.
27. Teichert-Kuliszewska K, Kutryk MJ, Kuliszewski MA, Karoubi G, Courtman DW, Zucco L, Granton J, Stewart DJ. Bone morphogenetic protein receptor-2 signaling promotes pulmonary arterial endothelial cell survival: implications for loss-of-function mutations in the pathogenesis of pulmonary hypertension. *Circ Res*. 2006;98:209–217.
28. Machado RD, Pauciulo MW, Thomson JR, Lane KB, Morgan NV, Wheeler L, Phillips JA, Newman J, Williams D, Galiè N, et al. BMPR2 haploin-sufficiency as the inherited molecular mechanism for primary pulmonary hypertension. *Am J Hum Genet*. 2001;68:92–102.
29. Thomson JR, Machado RD, Pauciulo MW, Morgan NV, Humbert M, Elliott GC, Ward K, Yacoub M, Mikhail G, Rogers P, et al. Sporadic primary pulmonary hypertension is associated with germline mutations of the gene encoding BMPR-II, a receptor member of the TGF-beta family. *J Med Genet*. 2000;37:741–745.
30. Lane KB, Machado RD, Pauciulo MW, Thomson JR, Phillips JA III, Loyd JE, Nichols WC, Trembath RC; The International PPH Consortium. Heterozygous germline mutations in BMPR2, encoding a TGF-beta receptor, cause familial primary pulmonary hypertension. *Nat Genet*. 2000;26:81–84.
31. Costello CM, Howell K, Cahill E, McBryan J, Konigshoff M, Eickelberg O, Gaine S, Martin F, McLoughlin P. Lung-selective gene responses to alveolar hypoxia: potential role for the bone morphogenetic antagonist gremlin in pulmonary hypertension. *Am J Physiol Lung Cell Mol Physiol*. 2008;295:L272–L284.
32. Myllarniemi M, Vuorinen K, Pulkkinen V, Kankaanranta H, Aine T, Salmenkivi K, Keski-Oja J, Koli K, Kinnula V. Gremlin localization and expression levels partially differentiate idiopathic interstitial pneumonia severity and subtype. *J Pathol*. 2008;214:456–463.
33. Koli K, Myllarniemi M, Vuorinen K, Salmenkivi K, Ryynanen MJ, Kinnula VL, Keski-Oja J. Bone morphogenetic protein-4 inhibitor gremlin is overexpressed in idiopathic pulmonary fibrosis. *Am J Pathol*. 2006;169:61–71.
34. Kariyawasam HH, Xanthou G, Barkans J, Aizen M, Kay AB, Robinson DS. Basal expression of bone morphogenetic protein receptor is reduced in mild asthma. *Am J Respir Crit Care Med*. 2008;177:1074–1081.
35. Richter A, Yeager ME, Zaiman A, Cool CD, Voelkel NF, Tuder RM. Impaired transforming growth factor-beta signaling in idiopathic pulmonary arterial hypertension. *Am J Respir Crit Care Med*. 2004;170:1340–1348.
36. Southwood M, Jeffery TK, Yang X, Upton PD, Hall SM, Atkinson C, Haworth SG, Stewart S, Reynolds PN, Long L, et al. Regulation of bone morphogenetic protein signalling in human pulmonary vascular development. *J Pathol*. 2008;214:85–95.
37. Jeffery TK, Upton PD, Trembath RC, Morrell NW. BMP4 inhibits proliferation and promotes myocyte differentiation of lung fibroblasts via Smad1 and JNK pathways. *Am J Physiol Lung Cell Mol Physiol*. 2005;288:L370–L378.
38. Atkinson C, Stewart S, Imamura T, Trembath RC, Morrell NW. Immunolocalisation of BMPR-II and TGF-β type I and II receptors in primary plexogenic pulmonary hypertension. *J Heart Lung Transplant*. 2001;20:149.
39. Hong JH, Lee GT, Lee JH, Kwon SJ, Park SH, Kim SJ, Kim IY. Effect of bone morphogenetic protein-6 on macrophages. *Immunology*. 2008;128:e442–e450.
40. Pugliese SC, Kumar S, Janssen WJ, Graham BB, Frid MG, Riddle SR, El Kasmi KC, Stenmark KR. A time- and compartment-specific activation of lung macrophages in hypoxic pulmonary hypertension. *J Immunol*. 2017;198:4802–4812.

41. Sha G, Zhang Y, Zhang C, Wan Y, Zhao Z, Li C, Lang J. Elevated levels of gremlin-1 in eutopic endometrium and peripheral serum in patients with endometriosis. *Fertil Steril*. 2009;91:350–358.
42. Sneddon JB, Zhen HH, Montgomery K, van de Rijn M, Tward AD, West R, Gladstone H, Chang HY, Morganoth GS, Oro AE, et al. Bone morphogenetic protein antagonist gremlin 1 is widely expressed by cancer-associated stromal cells and can promote tumor cell proliferation. *Proc Natl Acad Sci USA*. 2006;103:14842–14847.
43. Namkoong H, Shin SM, Kim HK, Ha SA, Cho GW, Hur SY, Kim TE, Kim JW. The bone morphogenetic protein antagonist gremlin 1 is overexpressed in human cancers and interacts with YWHAH protein. *BMC Cancer*. 2006;6:74.
44. Liu Y, Li YC, Hou RZ, Shu Z. Knockdown grem1 suppresses cell growth, angiogenesis, and epithelial-mesenchymal transition in colon cancer. *J Cell Biochem*. 2019;120:5583–5596.
45. Kim M, Yoon S, Lee S, Ha SA, Kim HK, Kim JW, Chung J. Gremlin-1 induces BMP-independent tumor cell proliferation, migration, and invasion. *PLoS One*. 2012;7:e35100.
46. De Jesus DS, Devallance E, Li Y, Falabella M, Guimaraes D, Shiva S, Kaufman BA, Gladwin MT, Pagano PJ. Nox1/Ref-1-mediated activation of CREB promotes Gremlin1-driven endothelial cell proliferation and migration. *Redox Biol*. 2019;22:101138.
47. Maciel TT, Melo RS, Campos AH. The bone morphogenetic protein antagonist gremlin promotes vascular smooth muscle cell apoptosis. *J Vasc Res*. 2009;46:325–332.
48. Wellbrock J, Harbaum L, Stamm H, Hennigs JK, Schulz B, Klose H, Bokemeyer C, Fiedler W, Lüneburg N. Intrinsic BMP antagonist gremlin-1 as a novel circulating marker in pulmonary arterial hypertension. *Lung*. 2015;193:567–570.

SUPPLEMENTAL MATERIAL

Figure S1. Flow chart showing the number, grouping and RHC procedure performed in rats received CSG.

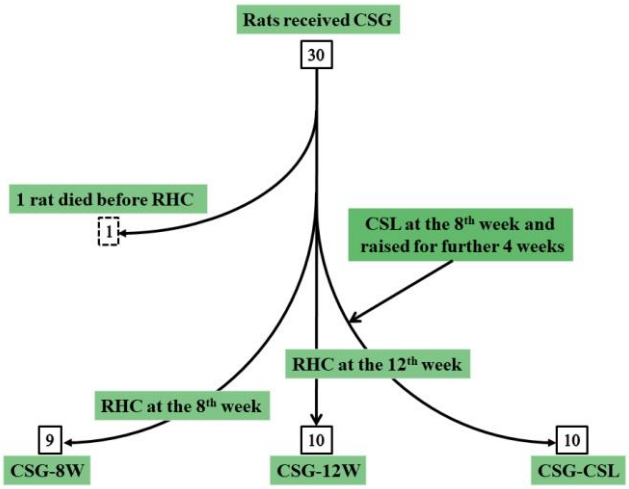

CSG: combined surgery group; RHC: right heart catheterization; CSL: cervical shunt ligation.

Figure S2. mRNA level of gremlin-1 in lungs from SOG and CSG.

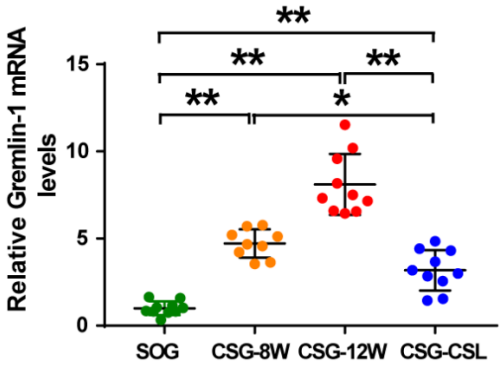

Data are mean ± SD. n = 9 – 10 rats pre group. $^{**}P$ <.01. SOG: sham operation group; CSG-8W: combined surgery group reserving for 8 weeks; CSG-12W: combined surgery group reserving for 12 weeks; CSG-CSL: combined surgery group receiving cervical shunt ligation at the postoperative 8th week and continuously kept for the subsequent 4 wk.

Figure S3. Gremlin-1 antagonized the inhibitory effect of BMP4 on dPASMCs proliferation.

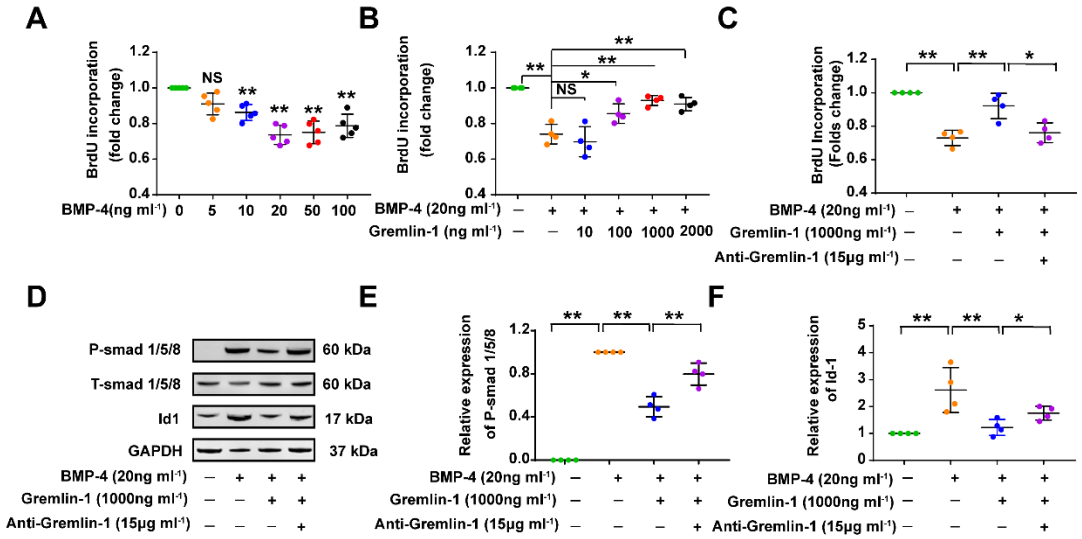

(A). BMP4 concentration-dependently inhibitory dPASMCs proliferation and reached the maximal effect at 20ng/ml; **(B).** Gremlin-1 concentration-dependently antagonized the anti-proliferative effect of BMP4 (20ng/ml) on dPASMCs and achieved the maximally antagonistic effect at 1000ng/ml; **(C).** Anti-gremlin-1 (15μg/ml) reversed the maximally antagonistic effect of gremlin-1 (1000ng/ml) for BMP4 (20ng/ml); **(D-F).** Representative Western-blotting image and densitometric analysis showing that BMP4 (20ng/ml) induced significant Smad1/5/8 phosphorylation **(D, E)** and Id1 expression activation **(D, F)** in dPASMCs, which was apparently antagonized by gremlin 1 (1000g/ml) and reversed by additional anti-gremlin-1 (15μg/ml). Data are mean ± SD of 4-5 independent experiments. $^{**}P<0.01$, $^{*}P<0.05$ and $^{NS}P>0.05$. BMP-2: bone morphogenetic protein-2; Id1: inhibitor of DNA binding 1.

Figure S4. Gremlin-1 blocks the pro-apoptotic effects of BMP4 on dPASMCs.

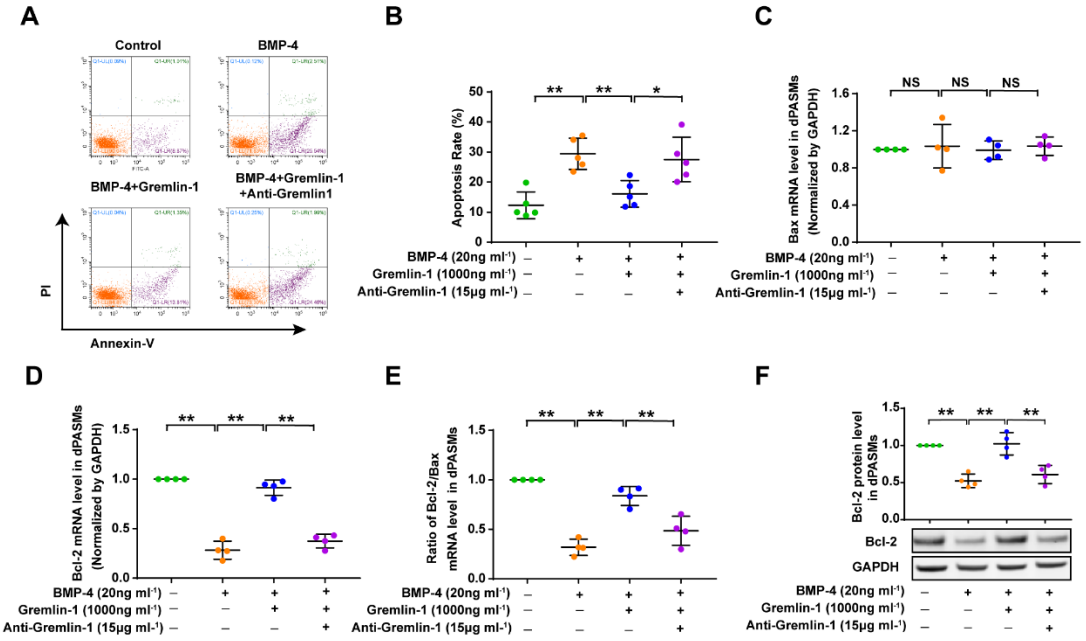

(A). Representative flow cytometry images showing the effects of BMP4, BMP4 + gremlin-1, BMP4 + gremlin-1 + anti-gremlin-1 on the apoptosis of dPASMCs; **(B).** Quantification of apoptotic cells; **(C-F).** Effect of BMP4, BMP4 + gremlin-1, BMP4 + gremlin-1 + Anti-gremlin-1 on Bax mRNA level **(C)**, Bcl-2 mRNA level **(D)**, ratio of Bcl-2/Bax **(E)** and Bcl-2 protein level **(F)** in dPASMCs. Data are mean ± SD of 4-5 independent experiments. $^{*}P < .05$, $^{**}P < .01$ and $^{NS}P > .05$ vs. control group. Bcl-2: B-cell lymphoma-2; BMP-4: bone morphogenetic protein-4.